

DEFORMATION-INDUCED MASS TRANSFER IN FELSIC VOLCANIC ROCKS HOSTING THE BRUNSWICK NO. 6 MASSIVE-SULFIDE DEPOSIT, NEW BRUNSWICK: GEOCHEMICAL EFFECTS AND PETROGENETIC IMPLICATIONS

DAVID R. LENTZ¹

New Brunswick Geological Surveys Branch, Department of Natural Resources and Energy, P.O. Box 50, Bathurst, New Brunswick E2A 3Z1 and Department of Geology, University of New Brunswick, Fredericton, New Brunswick E3B 5A3

ABSTRACT

Four samples of felsic volcanic rocks, footwall to the Brunswick No. 6 massive sulfide deposit, in the Bathurst area of New Brunswick, were analyzed to assess the chemical effects of solution transfer during the development of a fabric (composite S_1/S_2 , septa/folia). Wide-beam electron-microprobe traverses across the domainal fabric show no obvious chemical change within the microlithons. Using Al as a conserved element, mass balance of the averaged contents principally show Si and Zn (\pm Na) removal from the septa relative to the microlithons, with some notable changes in Fe, Mg, Mn, Na, and K. Whole-rock compositions of separates of the microlithons and septa show major-element changes similar to the mass-balanced microprobe data, although there were no significant mass changes involving trace elements, except Zn. However, individual samples exhibit some trace-element mobility ($< 50\%$), in particular the light-rare-earth elements (< 50 to 150%). Values of $\delta^{18}\text{O}$ are lower in the septa than in the microlithons, on average -0.13% per 1 wt.% SiO_2 (depletion) within the septa. On the basis of an estimated solubility of silica (1 wt.%) and a small degree of silica unsaturation (80% saturated), a minimum fluid:rock ratio (F/R) of 50 is required to produce these septa *via* solution transfer, assuming the microlithons were unchanged. This situation requires the removal and transport (open system) of chemical constituents, mainly silica. Alternatively, if the microlithons were changed during deformation, the F/R would be proportionally lower, with constituents (mainly silica) locally redistributed owing to pressure differentials between the septa and microlithons (*i.e.*, closed system). The relative homogeneity of the microlithons and mobility of silica (among other constituents) to form regional quartz veins here and from numerous other localities documented in the literature indicate that the F/R was relatively high, favoring considerable open-system mass transport. The isotopically light, possibly cooler metamorphic fluids (-1 to 7%) were probably derived at depth in the accretionary wedge (Brunswick subduction complex).

Keywords: element mobility, mass transfer, pressure solution, fabric, foliation, cleavage, differentiated layering, massive sulfide, Brunswick, Bathurst, New Brunswick.

SOMMAIRE

Quatre échantillons de roche volcanique de composition felsique, formant le socle du gisement de sulfures massifs dit Brunswick No. 6, dans la région de Bathurst, au Nouveau-Brunswick, ont été analysés afin d'établir le bilan des effets de transfert de solutions au cours du développement des éléments structuraux de la roche, par exemple la schistosité composite S_1/S_2 , les septums et la foliation. Des traverses avec une microsonde électronique à faisceau élargi de part et d'autre de ces domaines structuraux ne révèlent aucun changement évident au sein des microlithons. Si on accepte que l'aluminium a agi comme élément conservé, un bilan des masses moyennes démontre surtout le lessivage du silicium et du zinc (\pm Na) des septums par rapport aux microlithons, quoiqu'il y ait eu des changements appréciables en teneur de Fe, Mg, Mn, Na, et K. Les compositions globales des concentrés de microlithons et septums montrent des changements en teneur des éléments majeurs semblables à ceux qui semblent indiqués par les données obtenues à la microsonde électronique, quoique très peu de changements semblent avoir impliqué les éléments traces, sauf le Zn. Toutefois, certains échantillons font preuve d'une mobilisation partielle des éléments traces ($< 50\%$), en particulier les terres rares légères (< 50 à 150%). Les valeurs de $\delta^{18}\text{O}$ sont plus faibles dans les septums que dans les microlithons, en moyenne -0.13% par 1% de perte de SiO_2 (en poids) dans les septums. En supposant une solubilité de la silice de (1%, poids) et un faible degré de sous-saturation (80% du point de saturation), un rapport minimal de fluide à roche (F/R) de 50 semble nécessaire pour produire ces septums par transfert *via* une solution. On suppose que les microlithons sont restés inchangés. Cette situation requiert le lessivage et l'élimination de composants chimiques, surtout la silice, en système ouvert. Si au contraire les microlithons ont changé au cours de la déformation, le rapport F/R serait proportionnellement plus faible, avec les composants mobiles, surtout la silice, redistribués localement comme conséquence des différences en pression entre les septums et les microlithons (c'est-à-dire, en système fermé). L'homogénéité relative des microlithons et la mobilité de la silice (parmi les composants), menant à la

¹ E-mail address: dlentz@unb.ca

formation des veines de quartz d'importance régionale, ici et dans plusieurs localités décrites dans la littérature, indiquent que le rapport F/R était relativement élevé, ce qui a favorisé un transfert important en système ouvert. La phase fluide métamorphique, isotopiquement légère (–1 à 7‰) et possiblement à température plus basse, a probablement été dérivée à profondeur dans le prisme d'accrétion associé au complexe de subduction de Brunswick.

(Traduit par la Rédaction)

Mots-clés: mobilité des éléments, transfert de masse, solution sous pression, structure, foliation, clivage, différenciation métamorphique, sulfures massifs, Brunswick, Bathurst, Nouveau-Brunswick.

INTRODUCTION

Syndeformational metasomatism, accompanying dynamic metamorphism (Ague 1991, Erslev 1998) and fabric development (Kerrick 1977, McClay 1977, Rutter 1983, Etheridge *et al.* 1984, Bell & Cuff 1989, Cox & Etheridge 1989, Erslev & Ward 1994, Williams 1972, 1977, 1990), has long been recognized. However, the mechanisms of mobilization of major- and trace-element components, degree of volume change, and scale of mass transfer are not well understood. In particular, the degree of open- *versus* closed-system mass transfer of elements, *i.e.*, reorganization by local diffusion as opposed to net metasomatic mass-transfer (Kretz 1994), is contentious.

There have been numerous efforts to quantify the major- and trace-element chemical changes associated with regional metamorphism (Shaw 1954, 1956, Mueller 1967, Erslev 1998). Dehydration and decarbonation form integral parts of prograde metamorphism and concomitant deformation (Fyfe *et al.* 1978, Ferry 1994). These processes of volatile expulsion have the capacity to chemically modify the rock through metasomatic mass-transfer at the site where the fluids originate and then migrate to higher structural levels. The main problem with a calculation of the net mass-transfer in regional metamorphic sequences lies in ascertaining the original composition of a protolith. Therefore, it is very difficult to document statistically significant mass-transfer, even using mass-balance techniques, except for very obvious chemical effects.

The purpose of this contribution is to evaluate the major- and trace-element, and isotopic changes caused by solution-transfer-related fabric development in highly deformed felsic tuffs located in the footwall of the Brunswick No. 6 massive-sulfide deposit, New Brunswick (van Staal & Williams 1984, van Staal 1985, Lentz 1999). If these rocks are open systems, this study helps to quantify chemical changes resulting from deformation-induced mass transfer, which might help to assess other interpreted mineralogical and chemical changes experienced by the protolith prior to deformation.

BACKGROUND INFORMATION

The detailed study of major- and trace-element changes in shear zones provide a clearer picture of mass-

transfer because the protolith composition is more easily determined and the fluid:rock ratio (F/R) is relatively high (Kerrick *et al.* 1977, Condie & Sinha 1996). However, there are few studies on the chemical changes accompanying foliation development, and even fewer on trace-element behavior (Kerrick 1977, Glasson & Keays 1978, Stephens *et al.* 1979, Fueten *et al.* 1986, Bhagat & Marshak 1990, O'Hara & Blackburn 1989, Erslev & Ward 1994, Mancktelow 1994, Erslev 1998). Solution-precipitation creep (solution transfer for short) of SiO₂ is by far the most recognized and proposed chemical change associated with cleavage development (*e.g.*, Williams 1972, 1977, Beach 1974, 1977, 1979, Kerrich 1977, Kerrich *et al.* 1977, Fueten *et al.* 1986, Wright & Henderson 1992). In many cases, there is also a concomitant reduction in volume, with the development of a fabric consistent with other strain features and the regional formation of quartz-rich veins (open system). However, formation of differentiated layering (Williams 1977, 1990) by microscale reorganization of components between septa and microlithon (closed system) under approximately volume-constant bulk-deformation conditions should also be evaluated as an end-member hypothesis in any mass-transfer model (Bhagat & Marshak 1990, Wintsch *et al.* 1991).

The solubility of quartz and amorphous silica is well documented throughout the P–T range of most crustal metamorphic–metasomatic conditions (Walther & Helgeson 1977, Fournier 1985). It is known that intracrystalline strain can considerably enhance the solubility of quartz (Kerrick 1977, McClay 1977, Rutter 1983) such that the latter approaches that of amorphous silica. Also, an increase in incongruent solubility of SiO₂ in other silica-containing phases (feldspar, micas, *etc.*) may enhance the mobility of silica. Therefore, deformation involves a complex interplay between micro-scale processes (*e.g.*, plastic strain, recovery, and recrystallization, dissolution, diffusion, and nucleation–growth) and larger scale, metasomatic mass-transfer, in particular in the development of a fabric and in the formation of quartz (± feldspar, carbonate, sulfide, *etc.*) veins. If mass transfer is involved, then fluid–mineral equilibria and solute behavior are also critical considerations in the analysis of cleavage development (Wintsch 1985). Porosity and, in particular, permeability are considerably enhanced during the development of cleavage (Kerrick 1977, Fyfe *et al.* 1978, Etheridge *et al.* 1983).

Foliation septa may be important channelways that facilitate metamorphic dehydration and solution transfer, and hence should be characterized by a high fluid:rock ratio relative to the intervening microlithons. The commonly observed coarser grain-size of the septa minerals relative to those in the microlithons is also in part due to the presence and abundance of a free fluid phase (*e.g.*, as an aqueous grain-boundary film) facilitating growth through fluid-enhanced diffusion of the necessary components.

DESCRIPTION OF STUDY AREA AND SAMPLE SELECTION

The Brunswick No. 6 Zn–Pb–Cu–Ag deposit (van Staal & Williams 1984, van Staal 1985, 1987, Luff *et al.* 1993, Lentz 1999) located in the eastern part of the Bathurst Mining Camp, immediately overlies subaqueous pyroclastic flows and related volcanoclastic rocks of the late Arenig to Llanvirn Nepisiguit Falls Formation (van Staal & Fyffe 1995). These felsic volcanic rocks of the basal part of the Tetagouche Group overlie the Cambrian to Tremadocian sandstones, siltstones, and shales of the Miramichi Group (Fig. 1). Fine- to coarse-grained quartz–feldspar crystal tuffs occur at the base of the Nepisiguit Falls Formation, whereas remnants of stretched-out pumice and lithic fragments have been preserved in the upper part of the tuffaceous rocks of this volcanic unit, which is commonly phenoclast-free, particularly close to the massive-sulfide deposits.

Pretectonic seafloor hydrothermal alteration occurs to variable degrees in the upper part of the Nepisiguit Falls Formation directly beneath the orebodies (Lentz 1999). The seafloor alteration, which increases toward the Brunswick No. 6 deposit, is responsible for the variable silicification coincident with the alteration of feldspar phenocrysts and the groundmass of the rocks to a low-temperature assemblage of clays and micas. Bands of massive chlorite (chlorite schists) occur locally in the deformed tuffs close to the sulfide orebody (van Staal & Williams 1984).

Development of the spaced S_1 differentiated layering, with septa rich in phyllosilicates and microlithons rich in quartz (\pm feldspar, mica, sulfides), is pervasive throughout the area. The S_1 differentiated layering is folded by a large Z-shaped F_2 fold immediately south of the Brunswick No. 6 deposit and is overprinted by a more thinly spaced S_2 differentiated crenulation cleavage in the hinge region (Fig. 2, van Staal & Williams 1984, van Staal 1994). D_1 was accompanied by a moderate- to high-pressure chlorite- to biotite-grade greenschist-facies metamorphism (van Staal 1985). Peak biotite-grade metamorphism was achieved after D_1 , but before the end of D_2 , because biotite porphyroblasts grew across the S_1 , but are kinked and recrystallized during D_2 .

The best-developed differentiated layering (S_1) occurs in the footwall rocks to the deposit. This layering was axial planar to rare, originally recumbent F_1 folds

and consistently folded by upright F_2 structures (Fig. 2a). In contrast to the clear overprinting relationships between S_1 and S_2 in the F_2 fold hinges (Fig. 2a), age relationships are commonly ambiguous or absent on the F_2 limbs, mainly because S_2 is refracting on S_1 (Fig. 2b, see van Staal 1994). Where separation of the two cleavages is difficult or impossible, the main fabric has been mapped as a composite S_1/S_2 foliation. Quartz veins are generally strongly folded by F_2 (Fig. 3) and locally preserve abundant evidence of fibrous quartz–mica growths. Albite, and less commonly, alkali feldspar are present in the quartz-rich veins, particularly in or near rocks that contain feldspar. At least some of the feldspar is formed by hydrothermal precipitation with quartz in veins, because it also occurs in veins developed in feldspar-absent lithologies. This evidence suggests that there is a minor degree of hydrothermal mobilization of Al. Where preserved, the quartz–mica vein fibers are parallel to the L_1 extension lineation defined by segmented phenoclasts, strain shadows and fringes, and intragranular veins. Quartz veining continued during the rest of the deformation history (D_2 – D_4), but progressively to a much lesser extent consistent with decreased flux of fluid.

These samples were selected for this study because they have (1) a well-documented homogeneous composition in terms of immobile trace elements, (2) textural homogeneity, with a volcanic groundmass with variable degrees of silicification, and (3) a well-developed composite S_1/S_2 fabric that has been previously described in detail. The predeformational variability of composition of the rocks, due to seafloor alteration, has not significantly affected the mobility of elements with high ionic potential, which are relatively homogeneous, and typical of the volcanic protolith across the area. As will be illustrated later, the amount of silica present in the rock prior to deformation as a result of seafloor silicification appears to control the degree of mass (and volume) loss (calculated) of silica and other constituents during solution transfer. Therefore, this study also provides a test of the mobility of elements of high ionic potential against variable degrees of mass (and volume) loss associated with fabric development by comparing and contrasting mass-change effects. These attributes make this area particularly suitable for assessing element mobility during fabric development using mass-balance techniques.

PETROGRAPHY AND GEOCHEMICAL COMPOSITION

Petrographic observations

It is evident in hand specimen and thin section that the spaced S_1/S_2 fabric varies somewhat in intensity in each sample, although the spacing width remains relatively constant. From distal to proximal areas with respect to the deposit, samples 96–DL–17, 96–DL–18, 96–MC–819.6, and 96–MC–819.7 (Fig. 1) have

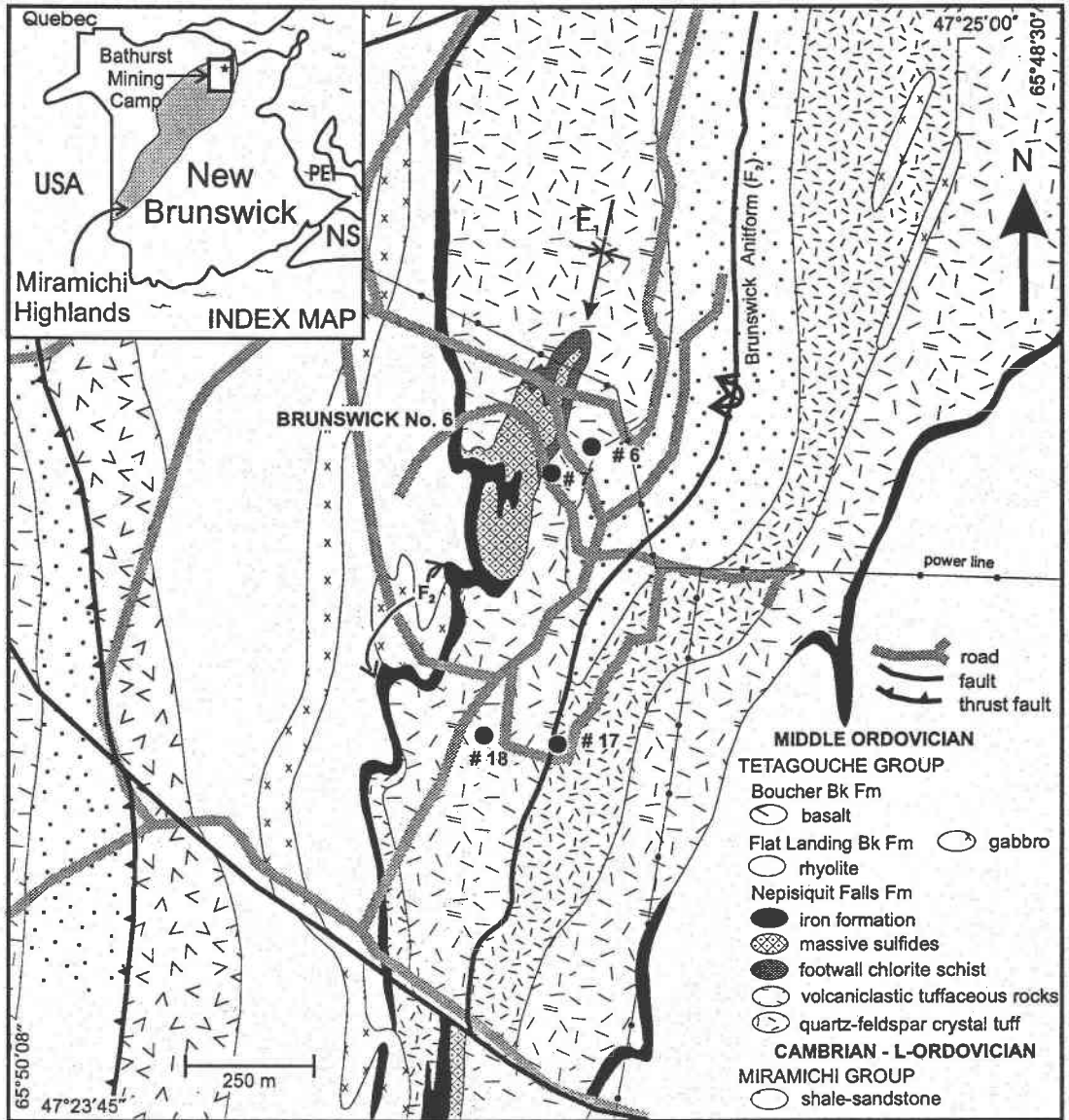


FIG. 1. Local geology around the Brunswick No. 6 massive sulfide deposit, with the locations of the samples discussed in this paper (modified after Boyle & Davies 1964, Luff *et al.* 1993). The inset shows the location in New Brunswick.

approximately 15–20%, 25%, 25–30%, and 25–30% septa, respectively. The microlithons are more leucocratic than the septa and have a relatively homogeneous mineral content.

Locally, the strongly altered and deformed crystal-poor tuffaceous sedimentary rock has preserved lapilli-like structures in the S_1 microlithons, the cores of which may be lapilli or least-altered protolith with outer silicic fringes (Fig. 2b). In the crystal-rich tuffs, the spacing of

S_1 and S_2 is generally significantly narrower and appears to be controlled by the size of the relict phenoclasts, around which the cleavage anastomoses. Quartz-rich strain shadows and mica beards occur around the quartz and feldspar phenoclasts that, together with the fibrous minerals in the intragranular veins in the pulled-apart phenoclasts, define a stretching lineation (Fig. 4). The marked differences in S_1 spacing and degree of anastomosing between the crystal-rich and crystal-poor tuffs

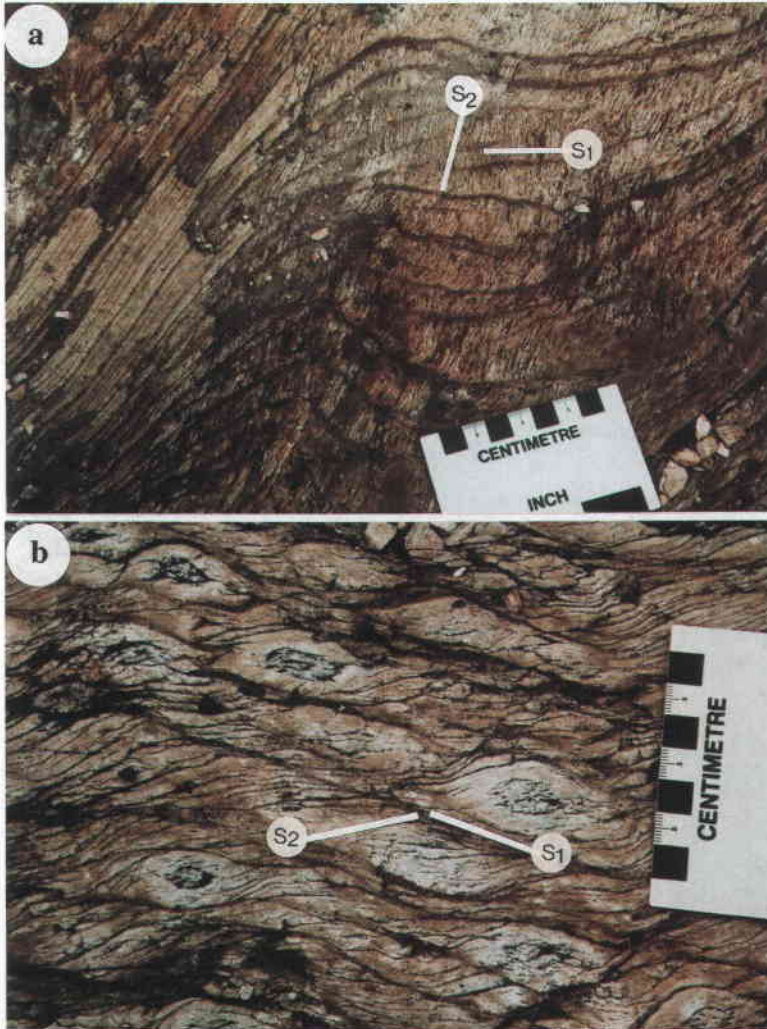


FIG. 2. a) Z-shaped F_2 fold in S_1 differentiated layering near sample 96-DL-18; see Fig. 1. Note that the S_2 axial planar cleavage (differentiated layering) is more narrowly spaced than S_1 in the hinge area, but becomes progressively indistinguishable from S_1 on the limbs, producing a composite S_1/S_2 cleavage. b) Refraction of narrowly spaced S_2 on more widely spaced S_1 differentiated layering at same location as (a). Lapilli-like (lapilli?), spongy siliceous material has preserved ellipsoidal areas between the intersecting foliations (septa).

probably reflect a predeformational mineralogical and textural difference in the variably altered (syngenetic, seawater-induced) felsic footwall sequence. Hence, the cleavage spacing is continuously diminished by a combination of progressive dissolution and brittle-plastic crystal strain accompanying the superimposed increments of deformation. In regional-scale shear zones (ductile thrusts, van Staal 1994), all the phenoclasts locally have been destroyed, and the rocks generally have

been transformed into mylonites or phyllonites. The meso- and microstructures indicate that the development of S_1 and S_2 was achieved by mobility of silica and, to a lesser extent, feldspar and other minerals. Dissolution of quartz and other minerals was less important in the microlithons compared to the septa. Hence, the degree of chemical change is probably also less than in the adjacent septa, but presumably not negligible, especially if silica is introduced into the microlithons. The domi-



FIG. 3. S_1 differentiated layering with parallel quartz-rich vein folded by F_2 and cut by tightly spaced S_2 fabric.

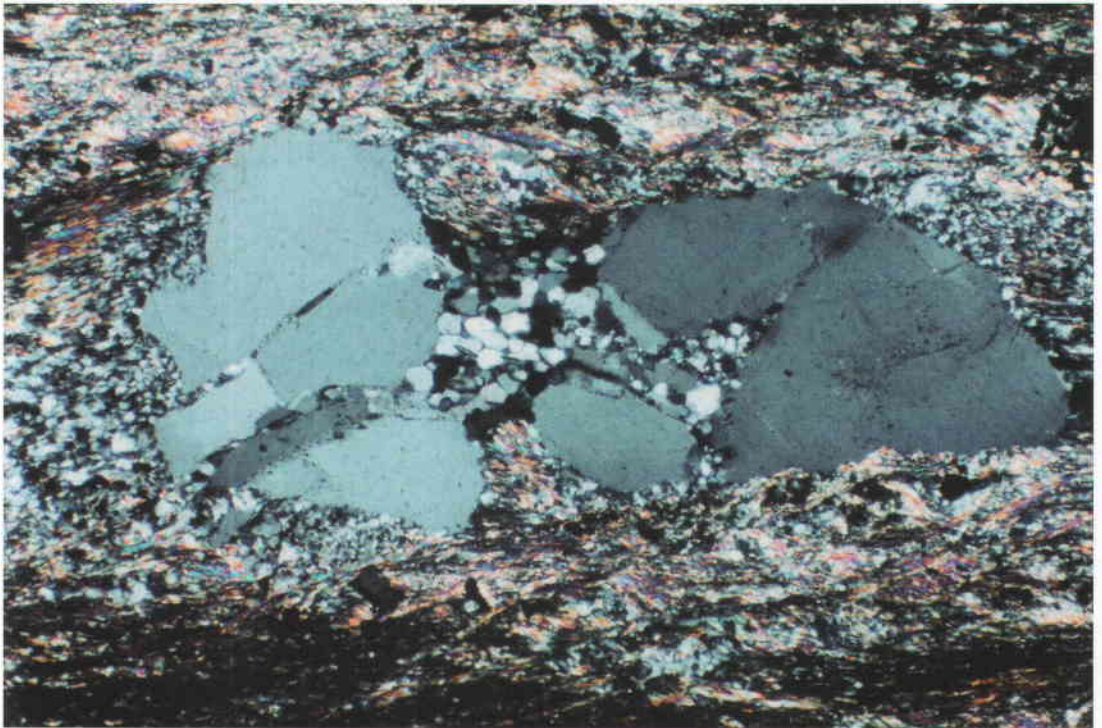


FIG. 4. Photomicrograph (cross-polarized light) of a quartz phenoclast or phenocryst (originally equant? like other phenocrysts) exhibiting selective dissolution parallel to the fabric (*i.e.*, flattened), an intragranular vein filled with quartz and quartz-rich pressure shadows. Field of view is 5.4 mm across.

nantly quartz-filled gashes (pull-aparts within the microlithons and phenocrysts) probably formed *via* local diffusion and redistribution of silica facilitated by a fluid phase (Ildefonse & Gabis 1976), as a result of local differentials in pressure (Gresens 1966) within the microlithon and between the microlithon and septa.

In general, the metamorphic grain-size of the chlorite, biotite, and phengitic white mica is greater within the septa than in the microlithons (Fig. 5). Other than the opaque phases, which are mainly sulfides, accessory phases (rutile, apatite, zircon) are estimated to be two to five times greater in grain size in the septa than within the microlithons, and are obviously more abundant. The coarser grain-size within the septa suggests that local fluid-enhanced diffusion was higher and that there were fewer nuclei.

Analytical methods

Polished thin sections were prepared for electron-microprobe analyses across a well-developed foliation layer in each of the four samples. The analyses (Table 1) were done using the JEOL-733 microprobe at the University of New Brunswick with 15 kV accelerating voltage and a 5 nA current, but with a broad beam (20 × 25 μm, to sample more material) and 80-second integration times. A combination of fused glass, mineral, and metal standards was used, with ZAF matrix corrections using CITZAF version 3.03. The analytical limits are on the order of 0.05 wt. %.

Separates of microlithon and septum (> 1.5 g) were made from each of four samples on a 5 cm × 5 cm block approximately 1 cm thick by hand crushing, followed

TABLE 1. AVERAGE MICROPROBE DATA WITH MASS-BALANCE ANALYSIS AND WHOLE-ROCK GEOCHEMICAL DATA

a) 97-DL-17								c) 96MC819.6							
n	Host	Fol't'n		RC	Δ	WR		n	Host	Fol't'n		RC	Δ	WR	
	41	1σ	14	1σ		1		29	1σ	10	1σ		1		
SiO ₂ (wt%)	79.26	8.66	44.38	9.08	28.96	-50.3	71.5	SiO ₂ (wt%)	67.35	17.21	36.93	15.82	24.18	-43.17	65.8
TiO ₂	0.180	0.168	2.196	2.267	1.43	+1.25	0.548	TiO ₂	0.084	0.085	0.069	0.086	0.045	-0.039	0.73
Al ₂ O ₃	11.16	4.83	17.01	2.759	11.16	0.00	13.1	Al ₂ O ₃	13.14	10.03	20.07	5.09	13.14	0.00	15.2
MgO	0.75	0.66	7.90	2.32	5.16	+4.41	1.88	MgO	0.98	0.83	4.08	1.47	2.67	+1.69	1.33
FeO	1.25	1.00	13.63	3.78	8.90	+7.65	3.10	FeO	5.72	5.23	24.06	8.26	15.75	+10.03	7.72
MnO	0.012	0.016	0.128	0.069	0.084	+0.072	0.02	MnO	0.023	0.030	0.123	0.076	0.081	+0.058	0.04
CaO	0.096	0.243	0.212	0.699	0.139	+0.127	0.22	CaO	0.054	0.048	0.031	0.018	0.020	-0.034	0.26
K ₂ O	2.97	2.01	7.52	2.12	4.91	+1.94	4.03	K ₂ O	3.58	3.32	2.46	1.06	1.61	-1.97	3.71
Na ₂ O	4.23	2.22	2.12	2.62	1.38	-2.85	2.79	Na ₂ O	0.19	0.14	0.14	0.08	0.09	-0.10	0.21
P ₂ O ₅	0.077	0.260	0.243	0.719	0.159	+0.082	0.15	P ₂ O ₅	0.028	0.025	0.016	0.024	0.010	-0.018	0.18
S	0.003	0.005	0.007	0.009	0.005	+0.002	0.010	S	0.005	0.008	0.006	0.007	0.004	0.001	0.59
Cl	0.019	0.015	0.067	0.027	0.044	+0.025	0.01	Cl	0.014	0.014	0.017	0.011	0.007	-0.007	0.007
Total	100.1		95.6				99.5	Total	91.3		89.3				99.2
Ba (ppm)	590	980	360	520	230	-360	635	Ba (ppm)	540	1010	170	350	110	-430	550
Zn	50	100	40	110	30	-20	45	Zn	60	110	230	180	150	90	781
Zr	90	180	70	110	50	-40	255	Zr	120	170	100	170	70	-50	325

$F_v = V^B/V^A = (X^A_{Al}/X^B_{Al}) * S^A/S^B = -46\%$ volume loss								$F_v = V^B/V^A = (X^A_{Al}/X^B_{Al}) * S^A/S^B = -46\%$ volume loss							
---	--	--	--	--	--	--	--	---	--	--	--	--	--	--	--

b) 96-DL-18								d) 96MC-819.7							
n	Host	Fol't'n		RC	Δ	WR		n	Host	Fol't'n		RC	Δ	WR	
	22	1σ	8	1σ		1		21	1σ	12	1σ		1		
SiO ₂ (wt%)	80.52	13.79	48.89	14.88	27.48	-53.04	72.5	SiO ₂ (wt%)	86.40	7.83	48.90	8.73	9.31	-77.09	68.6
TiO ₂	0.064	0.061	0.067	0.060	0.038	-0.026	0.326	TiO ₂	0.029	0.045	0.096	0.069	0.018	-0.011	0.53
Al ₂ O ₃	11.28	8.50	20.07	5.82	11.28	0.00	12.7	Al ₂ O ₃	4.52	3.38	23.75	4.15	4.52	0.00	13.0
MgO	0.30	0.19	2.28	0.85	1.28	+0.98	0.46	MgO	0.95	0.56	2.26	0.80	0.43	-0.52	1.81
FeO	1.84	1.43	17.78	6.18	10.00	+8.16	6.16	FeO	5.39	3.10	11.75	4.33	2.24	-3.15	8.44
MnO	0.006	0.012	0.118	0.050	0.066	+0.060	0.03	MnO	0.028	0.039	0.078	0.097	0.015	-0.013	0.05
CaO	0.021	0.018	0.041	0.020	0.023	+0.002	0.24	CaO	0.026	0.031	0.037	0.052	0.007	-0.019	0.06
K ₂ O	3.40	2.69	3.24	1.15	1.82	-1.58	2.98	K ₂ O	0.56	0.82	5.21	1.63	0.99	+0.43	2.51
Na ₂ O	0.13	0.09	0.15	0.06	0.08	-0.05	0.05	Na ₂ O	0.049	0.055	0.35	0.11	0.07	+0.021	0.13
P ₂ O ₅	0.010	0.013	0.021	0.021	0.012	+0.002	0.18	P ₂ O ₅	0.017	0.023	0.26	0.66	0.049	+0.032	0.06
S	0.004	0.006	0.003	0.005	0.002	-0.002	0.006	S	0.003	0.004	0.026	0.050	0.005	+0.002	0.22
Cl	0.005	0.007	0.013	0.009	0.007	0.002	0.01	Cl	0.002	0.004	0.004	0.005	0.001	-0.001	0.01
Total	97.6		92.7				99.1	Total	98.0		93.0				99.4
Ba (ppm)	330	490	110	190	60	330	410	Ba (ppm)	120	310	940	800	180	+60	440
Zn	60	140	100	270	60	0	45	Zn	60	110	380	1100	70	+10	687
Zr	70	120	70	130	40	-30	204	Zr	40	110	110	130	20	-20	249

$F_v = V^B/V^A = (X^A_{Al}/X^B_{Al}) * S^A/S^B = -53\%$ volume loss								$F_v = V^B/V^A = (X^A_{Al}/X^B_{Al}) * S^A/S^B = -84\%$ volume loss							
---	--	--	--	--	--	--	--	---	--	--	--	--	--	--	--

Notes: RC: reconstituted composition (CF*foliation), WR: whole-rock composition. CF is defined in the footnote to Table 2.

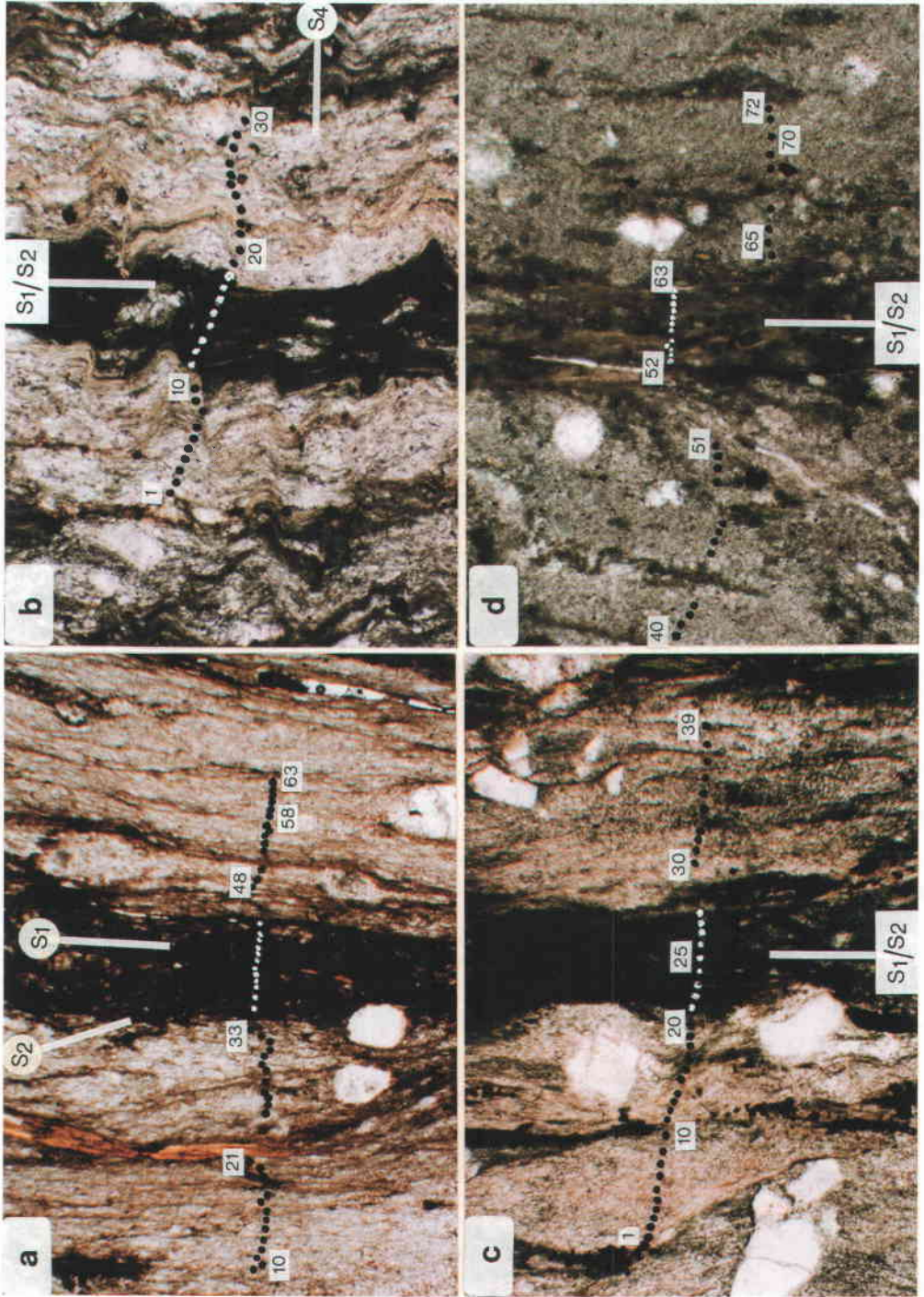


FIG. 5. Photomicrographs of septa (folia) and microlithons from each of the four samples selected; a) 96-DL-17, b) 96-DL-18, c) 96-MC-819.6, and d) 96-MC-819.7 in plane-polarized light. The points represent the wide-beam electron-microprobe traverses across the microlithon - foliation - microlithon boundary, with avoidance of quartz phenoclasts and accessory phases.

by separation with tweezers; hand pulverization was done using a mortar and pestle. These samples were analyzed with a Philips 2400 X-ray fluorescence (XRF) spectrometer using fused disks at the geochemical laboratory of the University of Ottawa (Table 2). The XRF integration times were increased to 180 seconds for all trace elements so as to increase the precision of the analyses. An in-house standard (94-RHY, Lentz 1995) indicated that the accuracy is within 2% for most major elements, but less than 10% for most trace elements, except for those with abundances approaching the detection limits. However, the precision of the analytical

results, which is most important in a mass-balance study of this kind, is less than 1% for virtually all elements, except P (2%), V (4%), Cr (7%), Co (38%), Ni (15%), Nb (3%), La (14%), Ce (7%), Nd (7%), Pb (2%), Th (3%), U (17%), and Ga (3%), on the basis of eight replicate analyses of the standard at a 95% confidence level.

The septa and microlithon separates for each of the four samples were analyzed for oxygen isotopes at the University of Western Ontario using the technique of Clayton & Mayeda (1963) and using an Optima mass spectrometer (Table 2). Sample precision and accuracy are approximately 0.2‰.

TABLE 2. MAJOR- AND TRACE-ELEMENT COMPOSITIONS OF THE WHOLE-ROCK, MICROLITHON, AND SEPTA WITH CALCULATED MASS-CHANGES FROM FOUR SAMPLE AREAS AT THE BRUNSWICK NO. 6 MASSIVE SULFIDE DEPOSIT, NEW BRUNSWICK

Sample	DL-17				DL-18				MC-6				MC-7				AVE
	WR	mln	septa	Δ													
SiO ₂ wt%	71.5	71.54	64.13	-19.25	72.5	75.08	66.56	-30.72	65.8	65.13	54.65	-19.46	68.6	72.31	62.9	-29.22	-24.70
TiO ₂	0.548	0.543	0.808	0.116	0.326	0.233	0.481	0.088	0.731	0.721	0.683	-0.150	0.527	0.437	0.612	-0.018	0.01
Al ₂ O ₃	13.1	12.82	15.71	0.00	12.7	10.67	16.01	0.00	15.2	14.33	17.15	0.00	13.0	10.69	15.61	0.00	0.00
Fe ₂ O ₃	3.44	3.53	5.07	0.60	6.84	7.54	7.81	-2.34	8.57	10.75	17.32	3.72	9.37	9.17	11.14	-1.54	0.11
MnO	0.02	0.032	0.053	0.011	0.03	0.045	0.045	-0.015	0.04	0.059	0.095	0.020	0.05	0.052	0.062	-0.010	0.00
MgO	1.88	1.83	2.72	0.39	0.86	0.90	0.96	-0.26	1.33	1.65	2.67	0.58	1.81	1.64	2.01	-0.26	0.11
CaO	0.22	0.31	0.51	0.11	0.24	0.20	0.32	0.01	0.26	0.26	0.27	-0.03	0.06	0.10	0.07	-0.05	0.01
Na ₂ O	2.79	3.06	2.92	-0.68	0.05	<0.10	<0.10	-	0.21	<0.10	<0.10	-	0.13	<0.10	<0.10	-	-0.17
K ₂ O	4.03	3.45	4.81	0.47	2.98	2.18	3.85	0.39	3.71	2.96	2.76	-0.65	2.51	1.84	3.05	0.25	0.11
P ₂ O ₅	0.15	0.169	0.191	-0.013	0.18	0.141	0.24	0.019	0.18	0.203	0.216	-0.023	0.06	0.074	0.056	-0.036	-0.01
LOI	1.7	1.4	1.9	0.1	2.3	2.3	2.9	-0.4	3.05	3.1	4.5	0.7	3.2	2.7	3.8	-0.1	0.1
SUM	99.5	98.9	99.1	-	99.1	99.3	99.3	-	99.2	99.4	100.5	-	99.4	99.2	99.6	-	-
Rb ppm	129	123	180	24	149	117	205	20	147	124	112	-30	116	96	157	12	6
Ba	635	509	648	19	412	328	562	47	552	443	410	-100	440	326	526	34	0
Sr	77	85	82	-18	9	6	11	1	24	16	16	-3	23	23	37	2	-4
Ga	14	14.7	20.6	2.1	13	11.4	21.3	2.8	18	18.0	23.2	1.4	16	13.5	18.8	-0.6	1.4
Nb	12	13	21	3	9	8	16	3	11	18	18	-3	9	12	16	-1	0
Th	14.0	14.5	19.4	1.3	11.0	9.2	16.2	1.6	20.0	17.5	17.6	-2.8	15.0	13.1	17.6	-1	-1
U	3.3	3.9	4.5	-0.3	5.7	3.5	5.8	0.4	3.5	1.9	0	-1.9	4.7	1.8	2.6	0	-0.5
Y	26	40	63	11	26	28	54	8	33	42	39	-9	36	33	45	-2	2
Zr	255	226	361	68	204	122	253	46	325	315	280	-81	249	198	268	-14	5
La	36.2	38	48	1	19.4	18	47	13	52.1	57	48	-17	38.5	35	45	-4	-2
Ce	79.5	101	126	2	44.7	26	99	40	115	117	108	-27	84	73	106	0	6
Nd	33.9	45	50	-4	21.1	14	44	15	54.3	50	43	-14	39.5	31	43	-2	-1
Pb	<2	21	20	-5	<2	<10	23	<15	38	10	11	-1	<2	8	10	-1	-1
Zn	45	51	80	14	45	44	49	-11	781	1014	481	-612	687	957	846	-377	-247
Cr	26	25	36	4	7	13	11	-6	29	31	31	-5	23	17	23	-1	-2
Ni	10	10	16	3	4	4	6	0	9	<1	6	<5	6	<2	2	<1	2
Co	5	4	9	3	5	4	6	0	12	9	12	1	11	10	15	0	1
V	47	46	72	13	17	13	20	0	53	50	56	-3	40	33	48	0	2
δ ¹⁸ O	-	11.83	10.79	-	-	9.54	8.60	-	-	7.89	7.31	-	-	7.85	5.86	-	-

Notes: WR: whole-rock (X-Ray Assay Ltd., Don Mills, Ontario), mln: microlithon (XRF, University of Ottawa), septa(e): foliation (XRF, University of Ottawa); Δ = (A*CF)-P, where A is the altered rock (foliation), P is parent (microlithon), and CF is the mass-balance correction factor (Al₂/Al₁), assuming aluminum is immobile (see text). This assumed immobility explains the Δ of Al₂O₃ is calculated as 0.00 (see above). The δ¹⁸O values are expressed in ‰ relative to standard mean ocean water (SMOW). LOI: loss on ignition.

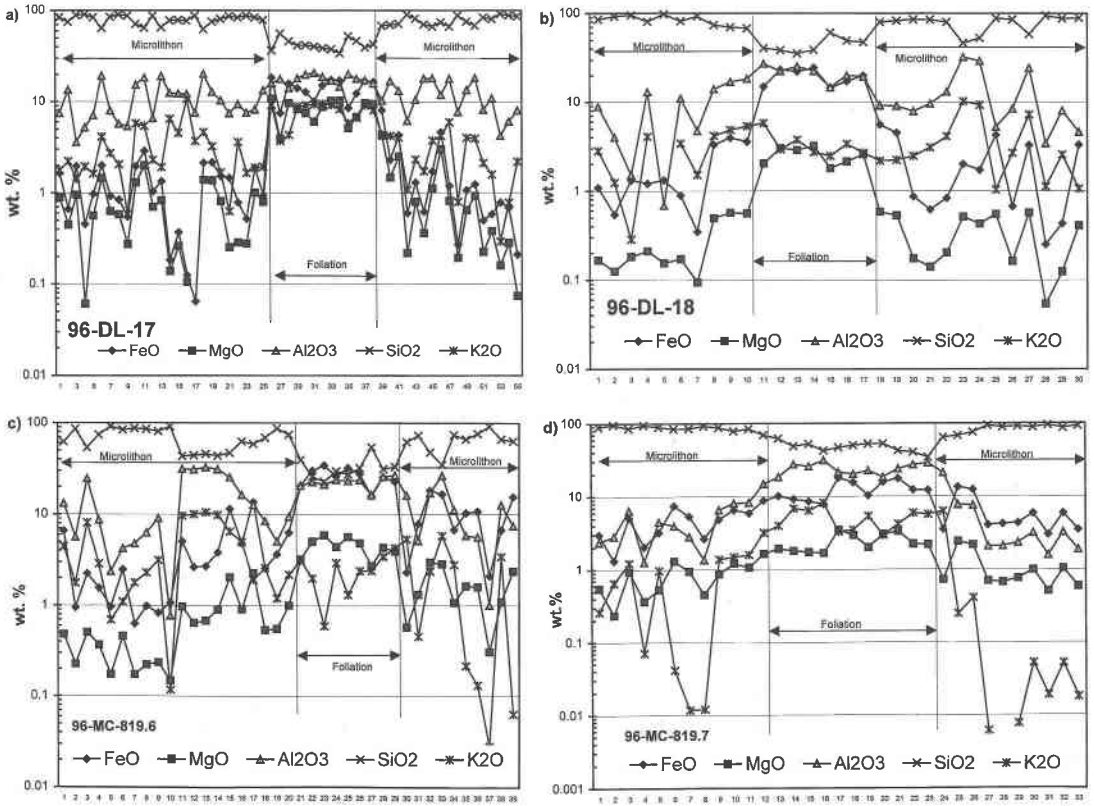


FIG. 6. Electron-microprobe compositional profiles for SiO₂, Al₂O₃, K₂O, FeO_T, and MgO across the microlithon – septa – microlithon boundaries of each of the four study samples. The data are deposited in CISTI (see text).

Constraints on foliation development: electron-microprobe results

An appropriate traverse was selected in each of the polished thin sections to document the compositional changes across a septum and both bounding microlithons. Table 1 presents the average chemical composition from the septum and microlithon for each traverse, and Figure 6 illustrates the raw geochemical variations along the traverses (data are deposited and available from the Depository of Unpublished Data, CISTI, National Research Council, Ottawa, Ontario K1A 0S2). Although somewhat variable, the profiles in Figure 6 illustrate that within the cleavage septum, the compositions are relatively uniform, reflecting their phyllosilicate mineralogy. Similarly, the bounding microlithons do not seem to show any obvious compositional gradient as the foliation septum is approached. The absence of gradients is inconsistent with a bulk volume-constant model of deformation, unless it is greater than the width of the microlithon. Although metasomatic changes may have affected the microlithons, for ex-

ample in the form of strain shadows and intragranular veins in the phenocrysts (Fig. 4), these changes were probably much less than those in the septa (Bell & Cuff 1989). Hence, we assume that the microlithon as a first approximation can be used as the “least-altered” precursor to the septum for the purpose of end-member calculations of the open-system scenario. Further constraints on these assumptions are discussed later.

Figure 7 illustrates the average compositions (Table 1) of the septa and microlithons. We calculated the mass balance assuming Al as the least mobile constituent (or monitor), justification for which will be discussed later. The microlithon compositions are closest to the whole-rock compositions, because they represent the higher volume-proportion of the rock. On the basis of relative Al contents of the microlithon and septum relative to the Al in the whole rock, the weight proportion of the septa, and the specific gravity estimates ($S^A/S^B = 0.83$), volume proportions of foliation can be estimated for each sample site; DL-17: 27 vol.%, DL-18: 13 vol.%, MC-6: 25 vol.%, and MC-7: 37 vol.%.

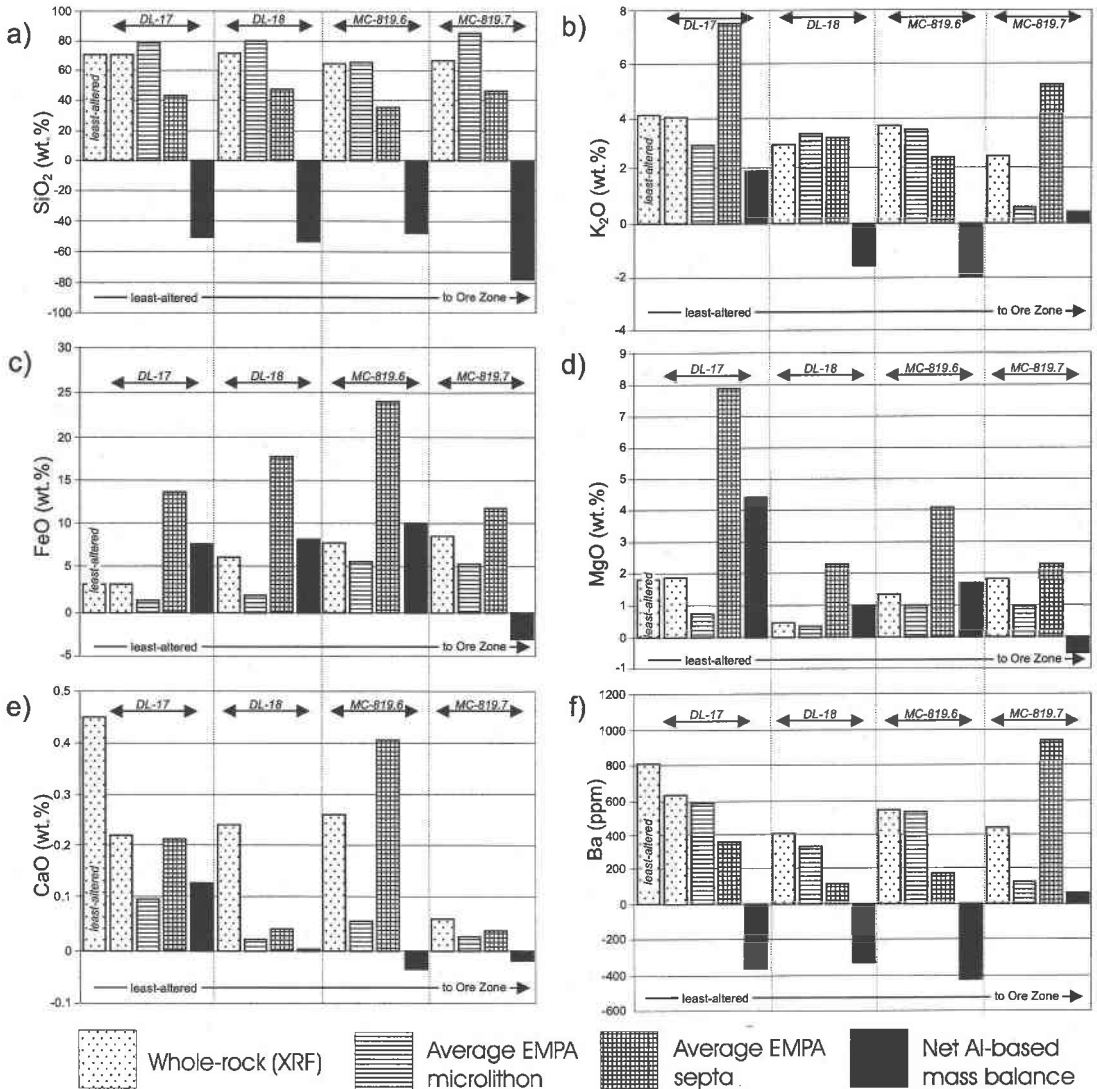


FIG. 7. Bar graph illustrating proportions of SiO₂, K₂O, FeO_T, MgO, CaO, and Ba for the average least-altered sample (Lentz & Goodfellow 1993) and, for each of the four samples studied, whole-rock composition (dots), average EMPA data for microlithons (horizontal lines), average EMPA data for foliations (cross-hatched), and net (Al-based) mass-balance (see Table 1).

The mass-change profiles illustrate the real changes associated with formation of the cleavage septa in contrast to the separations that are presented later. The composition of the two domains for each sample are also compared to the whole-rock data (Table 2). The composition of the least-altered sample (DL-17) is virtually identical to the average result of six whole-rock geochemical analyses (Lentz & Goodfellow 1993) from the homogeneous, least-altered, coarse-grained, quartz-feldspar crystal tuff.

Assuming Al “immobility”, the mass balance may be determined using the following equation (*cf.* Grant 1986):

$$\Delta X_i = W^B - W^A = [(X^A_{Al}/X^B_{Al}) * X^B_i] - X^A_i$$

where ΔX_i is the net change in mass for component *i*, W^A is the recalculated mass of the least-altered sample, X^A_i is the concentration of component *i* in the least-altered sample (A), X^B_i is the concentration of compo-

ment *i* in the altered sample (B), and X_{Al}^B/X_{Al}^A is the correction factor (CF). The specific gravities of the parent (S^A , microlithon) and altered (S^B , septa) samples were not determined in this study, although they should be on the order of 2.5 and 3.0 g/cm³, based on mineral assemblages, such that S^A/S^B equals approximately 0.83. The absolute weight-ratio (M^B/M^A) for the parent (M^A , microlithon) and altered (M^B , foliation) samples, together with the specific gravities, are used to calculate the volume factor (F_v) (Grant 1986):

$$F_v = V^B/V^A = (M^B/M^A)(S^A/S^B)$$

$$\text{with } M^B/M^A = X_{Al}^A/X_{Al}^B = CF$$

Therefore, the volume change associated with the development of the septa can be estimated (see Table 1).

On the basis of solubility of feldspar and muscovite – feldspar – quartz (Anderson & Burnham 1983, Walther & Woodland 1993), the [Al] is very low, *i.e.*, 0.0017 moles/L (\approx 46 ppm) at 400°C and 2.5 kbars, in contrast to silica, *i.e.*, 0.05 moles/L (\approx 3000 ppm) under the same conditions; therefore, Si is approximately 60 times more soluble than Al at these particular P–T and moderate pH conditions. Leitch & Lentz (1994) also pointed out that the solubility of a component must be considered in relation to its original abundance in the rock (*i.e.*, relative solubility index, RSI); the Al abundance is obviously very high relative to its solubility under most geological conditions considered here. The natural variance of a component also is a consideration, as well as the precision and accuracy of an analytical determination, in the selection of immobile elements. These considerations are important so as not to introduce errors in the calculated correction-factor (CF) that would be propagated through the calculation (Leitch & Lentz 1994). The calculated total variance and error in the whole-rock compositions of a suite of least-altered, coarse-grained, quartz–feldspar crystal-rich tuffs are within 3.0% at a 95% confidence level (Lentz & Goodfellow 1993). The precision and accuracy of Al₂O₃ concentrations are very good in both electron microprobe and whole-rock geochemical data, usually with less than 2% error. Nonetheless, Zr is also suspected to be even more immobile than Al (Erslev 1998), although its use as an immobile element monitor is not always practical owing to analytical problems and natural variance considerations.

On the basis of mass-balance calculations (Table 1), there is a considerable loss in volume (–46 to –84%) associated with the development of the differentiated layering, with the greatest losses associated with the most seawater-altered (silicified) sample near the deposit. Hence, the degree of volume loss seems to be directly proportional to the relative amount of silica present in the host protolith, which in this case is a siliceous chloritic tuff beneath the deposit. These losses in volume correspond to a considerable loss of silica from

the septum (43 to 77 wt.% SiO₂) relative to the microlithon, if the microlithon was closed (unaltered during deformation).

There are notable net increases in Fe (+7.65 to 10.0 wt.% FeO) in the septa in the three samples farthest from the deposit, but a net mass-loss of Fe (–3.2 wt.% FeO) in the sample closest to the deposit. Similarly, Mg has increased in the three most distal samples (to the deposit), but exhibits a net mass-loss (–0.5 wt.% MgO) in the most proximal sample. Potassium increases in the cleavage septa of the least-altered sample, probably owing to hydrolysis of feldspars to chlorite and phengite (now biotite), as evidenced by the depletion of Na (2.7 wt.% Na₂O); the remainder of the samples show virtually no change (+0.4 wt.% Na₂O) to a loss of 2 wt.% K₂O. The notable enrichments of Fe, Mg, and Mn in the three distal samples relative to their slight depletion in the most proximal, very altered sample have direct implications for synmetasomatic mass-transfer and exchange reactions in general.

Constraints on foliation development: XRF-determined bulk compositions

As previously mentioned, the microlithon and septum separates were prepared by hand; consequently, the XRF analyses lead to minimum determinations of mass balance compared to the electron-microprobe results. A comparison of the XRF-determined Al₂O₃ with the microprobe-determined value indicates an imperfect separation of the two domains: DL–17D: 72%, DL–17F: 78%, DL–18D: 112%, DL–18F: 54%, MC–6D: 83%, MC–6F: 58%, MC–7D: 68%, and MC–7F: 58% effective, calculated relative to the actual difference in the microprobe determinations of Al₂O₃. Nonetheless, the separations are such that the minor- and trace-element mobility can be assessed using the mass-balance approach. The compositions (XRF) of the microlithon (mln) and septum (s) for each of the samples are listed in Table 2.

The net change in mass (Δ , Table 2) was calculated by correcting the altered rock (septum) with the calculated correction-factor (CF) assuming that Al is immobile and comparing it to the parent (microlithon) as outlined earlier. The major-element changes in mass are generally similar to, but of lower magnitude than, those calculated using the electron-microprobe data; hence, the net mass-balances and volume-change calculations based on the electron-microprobe data are preferred. In each case, there is consistently a greater than 19 wt.% loss in SiO₂, which is about 2.5 times less than calculated from the electron-microprobe data.

In each of the samples, some changes in mass are evident and even involve some of the immobile trace elements: Ti, –21 to +21% (ave. = 2%); P, –49 to +13% (ave. 15%); Ga, –4 to 25% (ave. 10%); Nb, –17 to 38% (ave. = 0%); Th, –16 to 17% (ave. = 7%); Y, –21 to 29% (ave. = 6%); Zr, –26 to 38% (ave. 2%); La, –30 to

72% (ave. 5%); Ce, -23 to 154% (ave. 8%); Nd, -28 to 107% (ave. 3%); Cr, -46 to 16% (ave. = 9%), and V, -6 to 28% (ave. = 6%) (Table 2). The very low relative change in mass for all four samples based on the averages, except Zn, indicates that there is no obvious net flux of elements out of the system, except for SiO_2 . The locally high, net additions of high-ionic-potential elements, *e.g.*, Ti, P, Nb, Y, Zr, Th, and La, Ce, and Nd in sample DL-18, seem to be due to preferential growth of rutile, apatite, zircon, *etc.*, within the cleavage septa, because the bounding microlithons are significantly depleted in these components relative to their normal abundances in the rock. Metamorphic fluids infiltrating along the foliation planes probably enhanced local-scale diffusion of "immobile elements" such that new growth of trace phases is enhanced within the cleavage septa, particularly in sample DL-18. Net losses in mass, however, with no apparent change in the microlithons, *e.g.*, sample MC-6, imply that some leaching has occurred. If this is correct, then the local enrichment, albeit minor, of these same elements, *e.g.*, Ti, Ga, Nb, Y, and Zr in sample DL-17, could then be due to local hydrothermal saturation of Ti and Zr to form rutile and zircon.

Petrogenetic implications

It is evident that during fabric development, there seems to be some loss of SiO_2 coupled with variable alkali- and selected transition-metal exchange reactions. Compositional differences are evident between the microlithons and septa (Fig. 7). The strongest foliated rocks will have the most significant possible chemical changes, including a net decrease in SiO_2 if the systems were open. With a net loss in volume within the septum, there is an apparent increase in Al, as well as all relatively immobile elements. Analogous to what is found in most alteration studies, where volume-mass change is apparent, immobile-element ratios should be used in determining the composition of the rock protolith and in petrogenetic evaluations (Barrett & MacLean 1994, Leitch & Lentz 1994, Lentz 1996, 1998). For example, Figure 8a shows the apparent enrichment and depletion of immobile elements Ti and Zr; note that the ratio Zr/TiO_2 remains essentially the same despite the change in mass. Similarly, Nb and Y exhibit apparent changes between the microlithon and septum (Fig. 8b), such that they could skew the interpretation

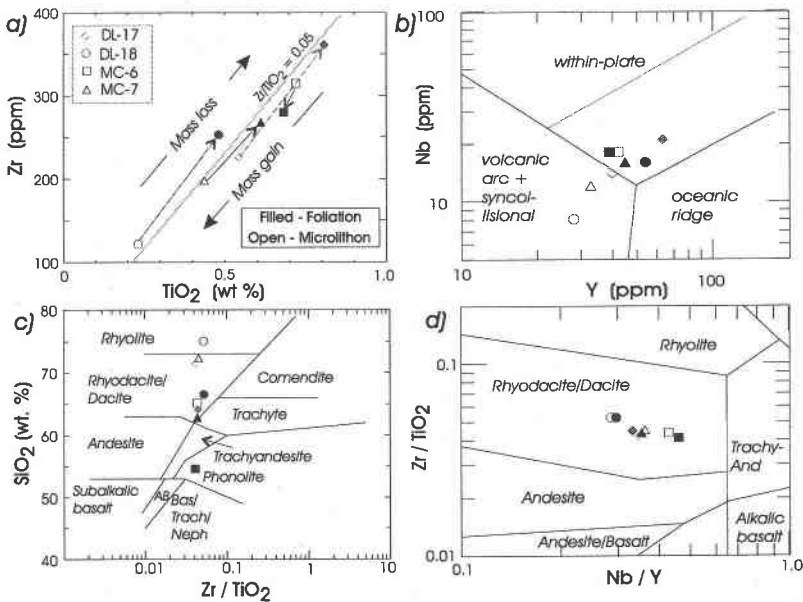


FIG. 8. a) Zr versus TiO_2 and b) Nb versus Y geotectonic-environment discrimination diagrams (Pearce *et al.* 1984), illustrating apparent changes in abundance due to mass loss or gain from the rock, although the Nb/Y values remain relatively unchanged (see d). Note that the original differences in abundance between each of the four microlithons (open symbols) are interpreted as a primary alteration-induced feature (dilution) due to original silicification and chloritization of the footwall system (see text for discussion). c) SiO_2 versus Zr/TiO_2 (Winchester & Floyd 1977), illustrating effect of solution transfer of silica from the foliation. d) Zr/TiO_2 versus Nb/Y compositional discrimination diagram (Winchester & Floyd 1977), showing the integrity of the immobile-element ratio systematics.

of geotectonic discrimination diagrams. The silica loss from the fabrics is independent of the Zr/TiO_2 variations (Fig. 8c), whereas there is virtually no detectable change in the Zr/TiO_2 or the Nb/Y values of the microlithon *versus* the septum, supporting the use of ratios of immobile elements in petrogenetic classification of metasomatically altered and deformed rocks (Winchester & Floyd 1977).

Oxygen isotope effects

There is a consistent $\delta^{18}O$ depletion (-0.58 to -1.99 ‰) between septum and microlithon that is associated

with a decrease in SiO_2 and exchange with metamorphic fluids. On average, there is a decrease in $\delta^{18}O$ of -0.127 ‰ per 1 wt.% SiO_2 depletion (Fig. 9). Since cleavage septa generally represent less than 25% of the volume of these rocks (see above estimates), the effect on whole-rock oxygen isotopes is generally in the order of 0.25‰ or less, if the microlithons did not exchange with metamorphic fluids. This scenario is probably unrealistic for these samples. However, there is some support for the inference that fluid exchange in the microlithons was less significant compared to the septa because the least-altered protolith (DL-17) has a $\delta^{18}O$ value of 11.83‰. This value is similar to what is ex-

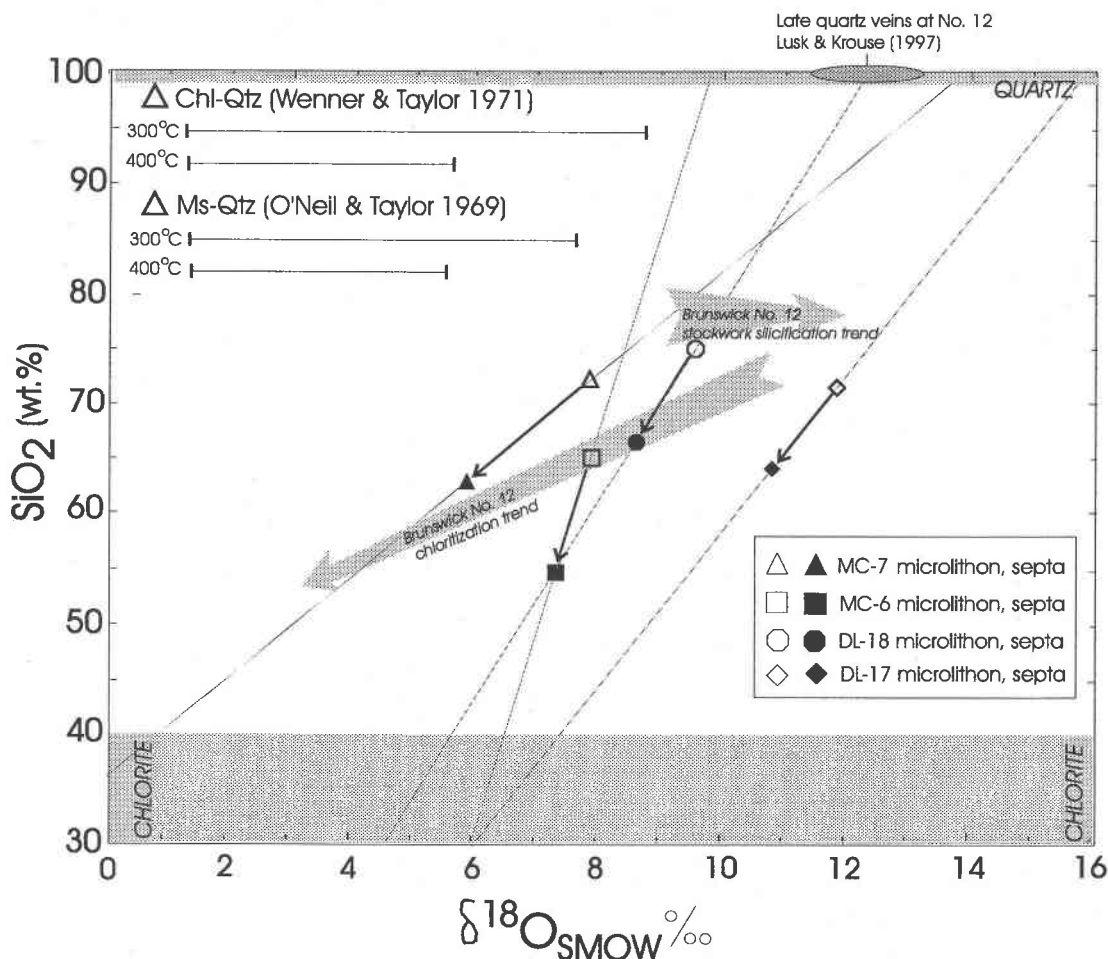


FIG. 9. $\delta^{18}O$ versus SiO_2 content of microlithon and septa samples. The extrapolated lines connecting each microlithon and septa sample are estimates of the possible O isotopic composition of chlorite separates that approximate fluid compositions, if in isotopic equilibrium. The trend for chloritization and stockwork silicification is inferred from Lentz & Goodfellow (1993, 1996). The silicification trend (No. 12) diverges from the chloritization trend, as cooling probably is involved. The four oxygen isotopic values of syntectonic quartz veins (Lusk & Krouse 1997) are similar to inferred (extrapolated) quartz end-member compositions of the microlithons and, possibly, mobilized silica from the septa. The degree of oxygen isotope fractionation between quartz and muscovite (O'Neil & Taylor 1969) and quartz and chlorite (Wenner & Taylor 1971) is illustrated.

pected for these weakly, synvolcanically altered felsic volcanic rocks, based on the quartz separates and matrix analyses in the Bathurst area (Lentz & Goodfellow 1993, 1996, Lentz *et al.* 1997, Lentz 1999). The decrease in $\delta^{18}\text{O}$ of the microlithons toward the massive sulfide deposit also is consistent with the progression toward more altered rocks approaching these deposits (Lentz & Goodfellow 1993, 1996, Lentz *et al.* 1997, Lentz 1999) and many other VMS systems.

If the septa samples were pure chlorite and in isotopic equilibrium with the microlithons, the samples would be approximately 7.5‰ (DL-17), 5.5‰ (DL-18), 6.5‰ (MC-6), and 1‰ (MC-7), based on extrapolation to 30–40 wt.% SiO_2 (Fig. 9). Considering that the chlorite– H_2O fractionation factor is approximately 0‰ in the 300° to 400°C range (Wenner & Taylor 1971), the estimated $\delta^{18}\text{O}$ values for chlorite approximate the isotopic composition of the metamorphic fluid. The more pronounced decrease in $\delta^{18}\text{O}$ with SiO_2 (MC-7, 0.21‰ per 1 wt.% SiO_2) is consistent with fluid exchange beginning at a lower temperature. The other three samples have inferred oxygen isotopic differences (septa–microlithon trends) consistent with equilibration in the 300° to 400°C range, although this does not necessarily indicate that the “equilibration” is syn- to post- D_1 metamorphism.

It is evident from the variable oxygen isotopic differences between septa and microlithon (*i.e.*, different slopes, Fig. 9) that these two domains are not always in isotopic equilibrium during their formation. The unusually light oxygen isotopic values of some of the septa imply partial equilibration with an egressing fluid.

Syntectonic quartz veins generated by these metamorphic fluids should have isotopic compositions similar to the extrapolated values of 100% SiO_2 contents, if deposited at the same temperature. Four syntectonic quartz veins sampled at the Brunswick No. 12 massive sulfide deposit yielded $\delta^{18}\text{O}_{\text{SMOW}}$ from 11.4 to 13.2‰ (Lusk & Krouse 1997), values that are close to those predicted (Fig. 9).

The inferred low $\delta^{18}\text{O}_{\text{fluid}}$ (–1 to 7‰, *i.e.*, like chlorite) cannot simply be explained by fluid flow and prograde metamorphic devolatilization at higher temperatures at depth (Dipple & Ferry 1992a, b), as the fluid would be heavier in ^{18}O than the inferred values based on simple partitioning equilibria. However, low-temperature devolatilization and fluid interaction may have begun at a lower P and lower T in the Brunswick subduction complex (van Staal 1994) to explain the inferred low $\delta^{18}\text{O}_{\text{fluid}}$. [Note added in proof: As indicated to me by Dr. Simon Peacock, Royden (1993) showed that reversed isotherms are possible in some accretionary wedge complexes, particularly in large and old ones, although it is equivocal whether or not the Brunswick Subduction Complex has the requisite characteristics. Such systems, with locally reversed geotherms related to subduction-related underplating of cooler, wet sedimentary and volcanic material during wedge development, may be responsible

for the high fluid:rock ratios noted, as well as the considerable mass-transfer evident in some ancient accretionary wedge complexes.]

DISCUSSION

Regional deformation of quartz-rich rocks, under low- to medium-grade metamorphic conditions and relatively slow strain-rates, is largely accommodated by extensive solution-transfer, which resulted in mass transfer. Channelized fluid-flow gave rise to high fluid:rock ratios locally, especially in shear zones and also along foliation planes. Owing to the strong evidence for solution transfer, local reorganization of components from the septa into the microlithons (*i.e.*, a closed system) has rarely been considered. An underlying assumption of the mass-transfer calculations and metasomatic inferences made herein is that the microlithons remained unchanged during deformation (*i.e.*, an open system). Reality, however, is probably somewhere between the open- and closed-system scenario (Fig. 10), which qualifies the remaining discussion. Assessing the mobility of elements impacting on mineralogical and whole-rock chemical changes is only relevant to the open-system mass-transfer scenario; the closed-system redistribution of components would not produce a change in bulk chemical composition during the formation of a fabric.

Considering the amount of silica leached from a rock through solution transfer in an open system, a rudimentary minimum estimate of fluid: rock ratio may be calculated assuming a specific value of silica solubility. Intracrystalline strain, however, may increase the solubility of quartz (Wintsch & Dunning 1985), possibly to such an extent that it approaches the significantly higher solubility of amorphous silica. For example, whereas the quartz solubility at 400°C and 600 MPa is on the order of 4 g/kg (Walther & Helgeson 1977), a reasonable estimate of the solubility of amorphous silica is about 10 g/kg (Fournier 1985). If we assume that the solubility of silica is like that of amorphous silica, *i.e.*, 10 g/kg (1 wt.% SiO_2) for the estimated P–T conditions (Fig. 11), net losses in mass of 43 to 77 wt.% SiO_2 within the septa suggest that the minimum fluid: fabric weight ratio is 43 to 77. These values are minimum estimates because the calculations are based on an upper estimate of the high solubility of silica and assume that the fluid is completely silica-unsaturated, whereas it is probably only weakly unsaturated at any point during its history. For example, high fluid: fabric ratios (>200) are suggested for the foliation and for the rock (F/R > 50 with 25% septa), if one assumes that the fluid was 20% undersaturated in silica. High F/R values have been documented elsewhere also, and are compatible with an integrated single-pass fluid flow through the system (Ferry 1994), particularly considering that D_1 was a progressive deformation resulting from continuous underthrusting of rocks beneath the Brunswick subduction complex (Fig. 11; van Staal 1994). Any solution-trans-

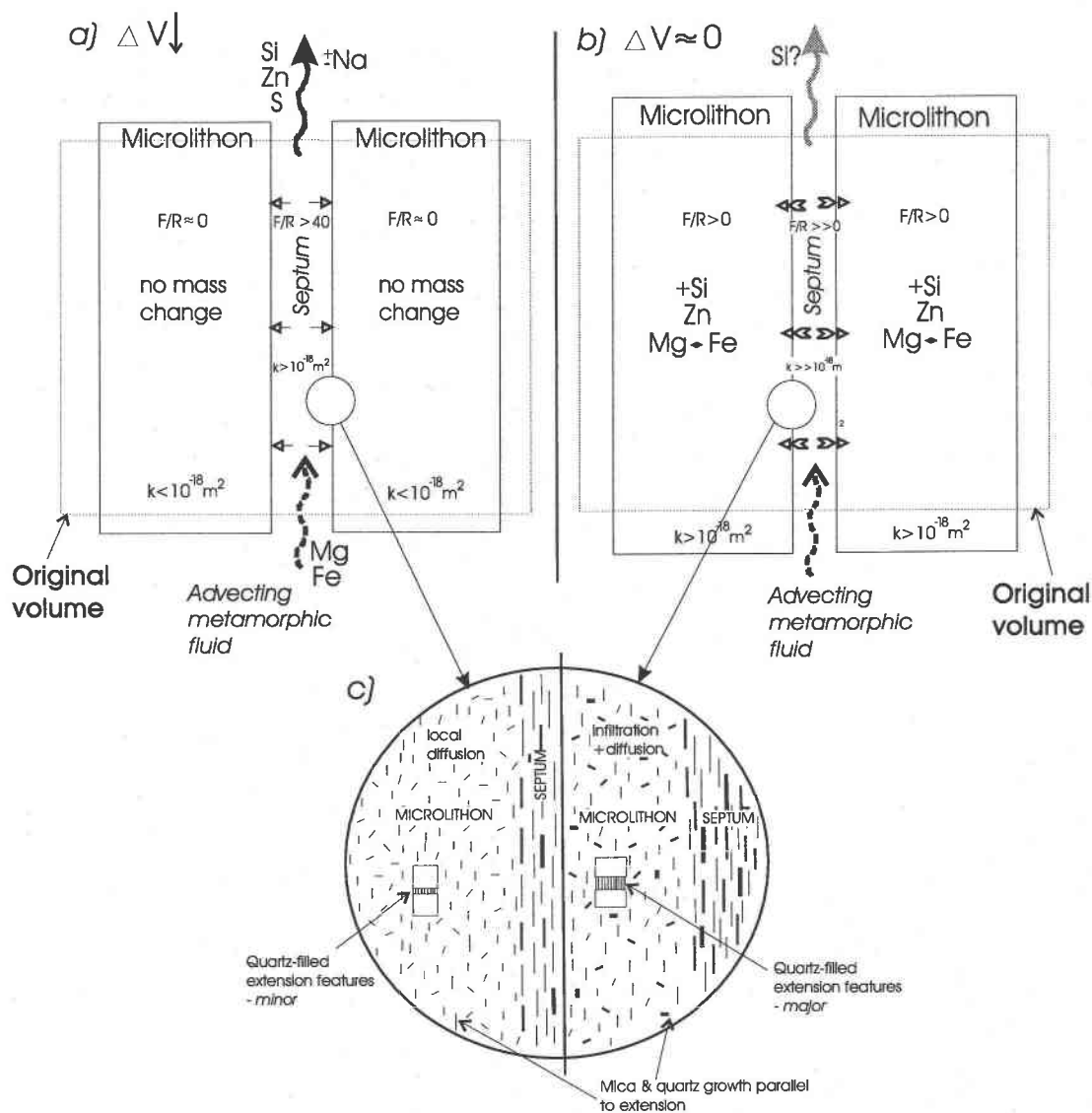


FIG. 10. Schematic diagram illustrating the various end-member mechanisms (open versus closed system) for foliation development and solution transfer of silica. a) Closed-system behavior of microlithons, *i.e.*, unaltered state during metamorphism and strain, demands open-system behavior of the septa in the rock as silica must have been removed completely *via* a buoyant metamorphic fluid. Extensional structures in the microlithon involve closed-system solution transfer (very local diffusion). b) Open-system behavior of microlithons during deformation and extension result in alteration. Instead of silica and other components being removed from the system, they can precipitate into extensional sites in microlithons, thus producing closed-system "differentiation" of the rock without mobilization of silica, *etc.* out of the system. c) Possible textural products of the two end-member scenarios within the microlithons. The relative permeabilities were estimated from discussions by Spear (1995).

fer fabric that forms during the early stages of D_1 is expected to be progressively enhanced by the continuous supply of aqueous fluid generated during dehydration of the newly underthrust rocks in this relatively

high pressure – low temperature environment of metamorphism. Hence solution-transfer fabrics are very well developed throughout the region (*e.g.*, van Staal & Williams 1984, de Roo & Williams 1990, Park 1996).

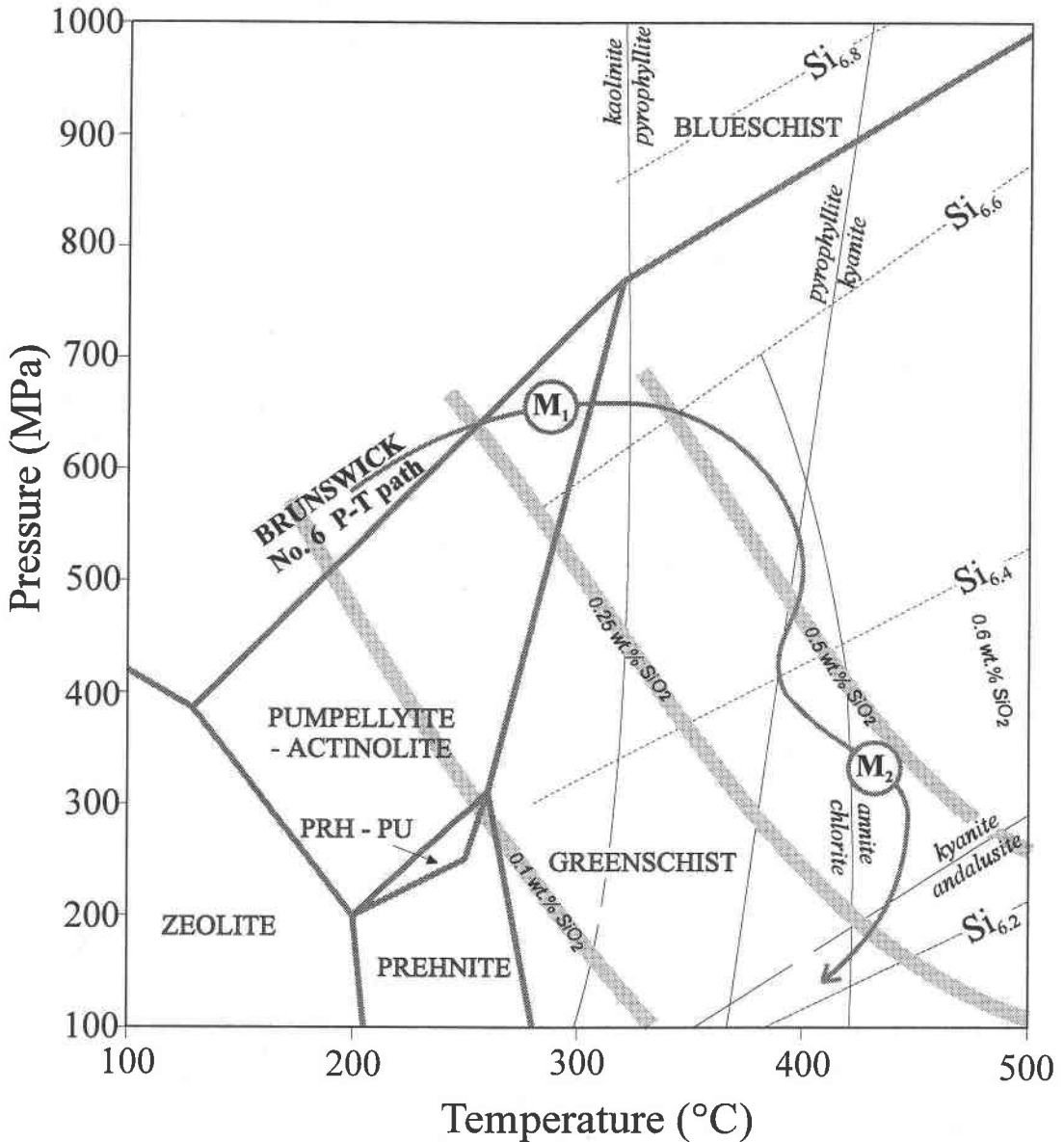


FIG. 11. Low-grade petrogenetic grid (after Bucher & Frey 1994) with superimposed P-T path of Tetagouche Group rocks in the Brunswick Mines area (modified from van Staal 1985, van Staal *et al.* 1990). The Si isopleths for the phengite geobarometer are presented (Massone & Schreyer 1987). The compiled hydrostatic solubilities of quartz are located (Fournier 1985).

The mass-balance calculations indicate that the cleavage septa generally have also been metasomatically enriched in Fe and Mg, which is mineralogically manifested by an increase of chlorite, phengite and biotite in the cleavage planes. The stability field of muscovite-phengite at a given activity of Fe and Mg, however, is enlarged at expense of feldspar, chlorite, and phlogo-

pite (biotite) in a fluid that is (presumably) slightly unsaturated in silica (Fig. 12) during the development of the fabric. Therefore, even higher activities of Fe and Mg in the infiltrating fluid are needed to stabilize chlorite in the septa during such conditions.

The occurrence of graphite within both the shales and footwall volcanic rocks of the Miramichi Group,

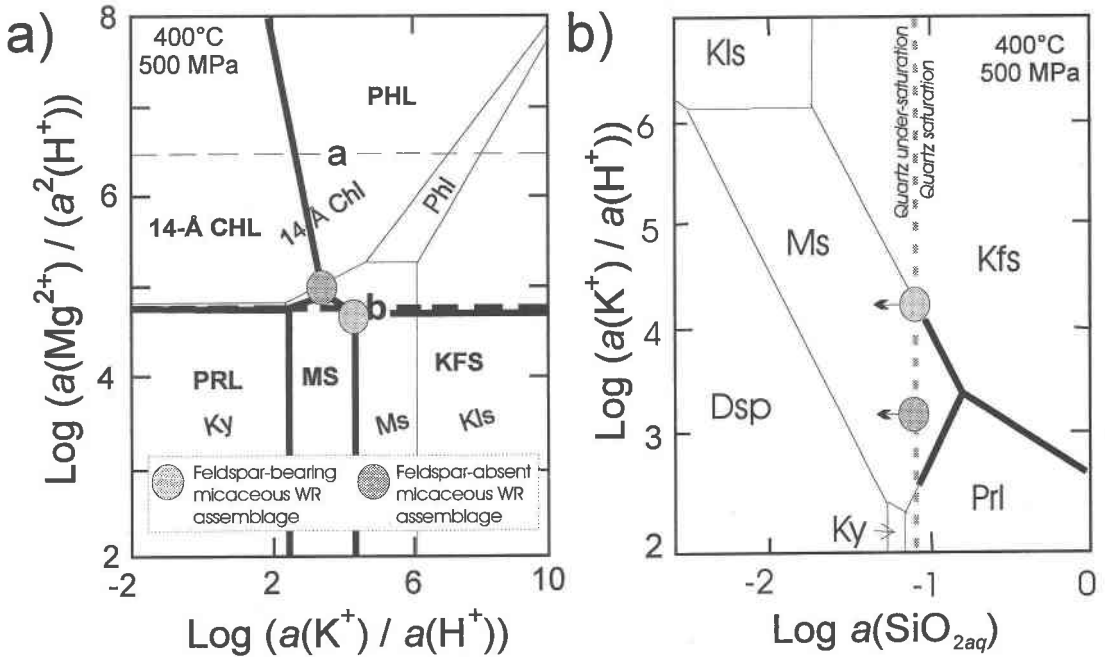
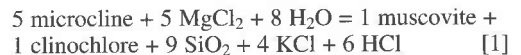


FIG. 12. $\log a(\text{Mg}^{2+})/a^2(\text{H}^+)$ (a), and $a(\text{SiO}_{2\text{aq}})$ (b) versus $\log a(\text{K}^+)/a(\text{H}^+)$ diagrams at 500 MPa and 400°C (after Bowers *et al.* 1984) illustrating the approximate stability of the Mg end-member phyllosilicates relative to muscovite (Ms) and alkali feldspar system (Kfs) (Mg–K–Si–Al–O–H) at quartz saturation (bold lines) and quartz undersaturation with kalsilite present (light lines). Symbols after Kretz (1983). The evolution from quartz-saturated to quartz-unsaturated (albeit weakly) conditions (arrows) enhances (slightly) the stability field of muscovite during pressure-solution development of the fabric.

particularly those that were syngenetically altered, will contribute some CO_2 – CH_4 – H_2S to the metamorphic fluid, such that it could reduce the $a(\text{H}_2\text{O})$ [*i.e.*, $P(\text{H}_2\text{O}) < P_T$ (Spear 1995)]. However, the high-pressure trajectory of the P–T path inhibits the hydrolysis of carbon ($\text{CH}_4 + \text{CO}_2$), hence the $P(\text{H}_2\text{O})$ was probably greater than 95% of P_T . This assertion is supported by the common presence of accessory minerals such as clinozoisite and titanite in the felsic volcanic rocks and interlayered mafic sills, magnetite coexisting with siderite in the overlying carbonate-facies iron formation, and abundant serpentine and talc in pre-tectonic, layered mafic–ultramafic sills in the felsic footwall sequence; these assemblages can only form at the ambient metamorphic conditions if $a(\text{H}_2\text{O})$ was very close to 1 (van Staal 1985). Metasomatic leaching or exchange reactions with rocks at deeper structural levels ultimately are responsible for the observed mass-additions of Fe and Mg, *e.g.*, muscovite formation at the expense of phengite under relatively acidic conditions can release Fe and Mg to the buoyant metamorphic fluid phase. This could be facilitated by the decrease in pressure and temperature of infiltrating buoyant solutions, resulting in dissociation of acid volatiles and H_2O . Similarly, the progressive hydrolysis of feldspars to muscovite (Gunter & Eugster 1980) also would result by the same process, releasing

silica and alkali metals to the metasomatic fluid. If the hydrolysis is coincident with Mg–Fe metasomatism, then metasomatic chlorite–muscovite assemblages could form (eq. 1) with net addition of Fe, Mg, and K, as is evident in the least-altered sample (DL–17).



Both these exchange reactions involved incongruent dissolution and mobility of silica if the fluid is unsaturated in SiO_2 during cleavage formation.

The chlorite from the fabrics in three feldspar-absent samples is chamositic (Chm 70 to 90), which corresponds to a $(\text{Fe}/\text{Mg})_{\text{fluid}}$ of approximately 100 (Saccocia *et al.* 1994). This high Fe activity, in part, reflects the nature of the seawater-altered host-rock near the deposit, but is also a function of fluid–mineral exchange equilibria (Eugster & Ilton 1983, Ilton & Eugster 1990).

Within the weakly mineralized footwall rocks to the massive sulfide deposit, the simple sulfide solubilities of pyrite, pyrrhotite, sphalerite (\pm galena, chalcopyrite), *etc.* are small, but significant under moderate-pH buffer conditions, *i.e.*, those approaching the pyrophyllite–muscovite buffer (pH in the range 3 to 4, depending on the $a(\text{K}^+)$). Interestingly, the simple solubility of pyrrho-

tite and magnetite is much higher than the solubility of pyrite and sphalerite (Crerar *et al.* 1978, Barnes 1979). The hydrostatic solubility of sphalerite at 400°C and pyrophyllite – muscovite – quartz buffer (0.5 M KCl) conditions yields approximately 2000 ppm Zn in solution (Hemley *et al.* 1967), but is much lower (500 ppm) at the K-feldspar – muscovite – quartz buffer, *i.e.*, a higher pH, and decreases to 50 ppm with increasing pressure to 200 MPa (Hemley *et al.* 1992). The hydrostatic solubility of Fe with the same assemblage at 400°C and 200 MPa (1 m Cl) is only about 200 ppm, and would be expected to decrease further with increasing pressure. Within feldspar-absent rocks, the appropriate buffers would be closer to the pyrophyllite – muscovite – quartz than the K-feldspar – muscovite – quartz buffer on the basis of the aluminous compositions of the chlorite, thus the solubilities (divalent metals) should be an order of magnitude higher. Therefore, the elevated activities of Fe may result from dissolution of pyrrhotite (\pm pyrite) by the metamorphic fluid in the footwall sequence *via* a solution reaction (eq. 2);



The incongruent desulfidation of pyrite to pyrrhotite with increasing temperature also should contribute to an increase of S_2 in the solution (Ferry 1981). The general absence of disseminated sulfides in the fabric elements attests to their mobilization. Pyrite, sphalerite, and chalcopyrite occur in the microlithons, with the coarsest varieties in extensional sites such as intragranular veins. If sulfides do occur in the septa, they seem, at least in part, to have grown relatively late (redistributed?), as they overgrow the S_1 cleavage locally. The leaching of Zn from the fabric, as indicated by both the microprobe- and XRF-based mass-balance calculations, suggests that Zn is more soluble than Fe. Fe preferentially partitions into the phyllosilicates with increasing temperature (Sverjensky 1985, Ilton & Eugster 1990). The solution of divalent metal sulfides (Cu, Pb, Zn, Ag, Au, *etc.*) is common during regional metamorphism of sedimentary sequences (Glasson & Keays 1978, Haack *et al.* 1984, Ague 1991), although a change in Zn is not evident in some cases (Roser & Nathan 1997).

Other than the high degree of silica mobility, the other components (Fe, Mg, Mn, K, Na, *LREE* and base metals) on average display relatively moderate changes in all four samples. Interestingly, Lusk & Krouse (1997) suggested that the salinity of the fluid inclusions in vein quartz at Brunswick No. 12 was moderate, approximately twice that of seawater, which could explain some of the mobility of Fe, Mg, Mn, Zn, and K and Na around Brunswick No. 6. These fluids will progressively change *via* reaction during their egress from the system, such that the chemical attributes of the fluids will not deviate significantly from the host (foliation) at any one instance, except along compositionally contrasting zones. It is conceivable that exchange reactions could also

occur within the microlithons *via* a fluid-assisted, grain-boundary mechanism of diffusion and microcracks, albeit probably at a lower F/R, thus altering them to a lesser degree than the septa (Fig. 10).

Immobile components

The mobility of many petrogenetically important elements during alteration and metamorphism has led to the use of immobile elements, particularly in volcanic and sedimentary rocks, to aid in their identification, petrochemical interpretation, and assignment of geotectonic environment. For the most part, cations with high charge and small radius (high ionic potential) are relatively insoluble in typical fluids under crustal P–T conditions, although $\text{Mg}(\text{OH})_2$ also is quite insoluble, but only at higher temperatures (>250 to 300°C). Jenner (1996) has compiled a list of the relative mobilities of elements with low to high ionic potential, including rare-earth elements (*REE*), and transition elements (*TE*). These empirical studies are generally focussed on low-pressure hydrothermal and metamorphic environments, although it is known that the solubility of hydroxide and alkali-hydroxide complexes is commonly prograde with pressure, as well as non-hydrostatic stress conditions (*e.g.*, Si, Al). A compilation of element mobilities in shear zones within granitic rocks (Condie & Sinha 1996) shows that Al, and many of the other elements of high ionic potential, generally exhibit little mass-change at temperatures less than 500°C (see also Roser & Nathan 1997). In this study, there is some evidence of minor mobility of high-ionic-potential elements, including light *REE* mobility, at least on the scale of separated septum and microlithon. The slight enrichment of Zr and Ti observed in DL-17 and DL-18 could be due to fluid-rock interaction with originally less-altered protoliths. On the other hand, the slight depletion in Ti and within the originally most-altered protoliths near the Brunswick No. 6 deposit, which also are characterized by a high degree of loss in silica and fabric development, implies that those elements may have been partially leached from the system. There is a pronounced similarity in relative enrichment or depletion of the high ionic potential elements, indicating: i) similar solubilities as hydroxide complexes [$\text{Zr}(\text{OH})_4$, $\text{Ti}(\text{OH})_4$, $\text{Y}(\text{OH})_3$, $\text{La}(\text{OH})_3$, *etc.*], *i.e.*, they have comparable solution and saturation behavior, ii) migration of high-ionic-potential elements, from the microlithons to the septa due to growth of trace phases within the septa, or iii) the sampling of the mica septa was not representative, a possibility that cannot be ruled out considering the relatively coarse-grained nature of accessory phases. The solubility of apatite, monazite, zircon, and rutile in high-P – high-T systems is generally very low, but rutile solubility is the highest (Ayers & Watson 1991, Van Baalen 1993). However, using the solubility formula for rutile, its solubility at 400°C and 600 MPa is only about 1 ppm in solution. Apatite and monazite solubilities increase

with decreasing pH (Ayers & Watson 1993, Wood & Williams-Jones 1994), but decrease with increasing temperature.

Our study indicates that the immobile elements, particularly their ratios (to avoid absolute mass-change effects), reasonably reflect the primary composition. Nevertheless, there is slight residual enrichment of immobile elements due to preferential dissolution of silica depending on the original quartz (\pm feldspar) content of the rock and the degree of fabric development. The residual enrichment of trace-element phases in the fabrics due to mass loss is well known. In this and other studies, the average grain-size of the phyllosilicates within the septa is generally greater than in the adjacent microlithons, indicative of enhanced grain-growth compared to the microlithons. Such enhanced grain-growth is facilitated by local diffusion, absence of other phases that inhibit growth, and presence of a fluid phase. Immobile elements in the septa, which are mainly contained in minerals susceptible to new growth, such as phyllosilicates, Ti-oxides (rutile, anatase, titanite), and epidote (allanite), may change their phase association (van Staal 1985), even though they may be relatively immobile on a microscale. However, Zr, which has a very low solubility, should not show new growth, thus commonly preserving its U–Th–Pb systematics. Nevertheless, van Staal (1985) noted that pulled-apart zircon crystals, as well as apatite, titanite, rutile, allanite, and epidote, are commonly filled in or overgrown by the same phases, indicating local, fluid-assisted, diffusion.

CONCLUSIONS AND RECOMMENDATIONS

Microstructural observations and electron-microprobe data across microlithon – septum – microlithon boundaries support the assumption that metasomatic modification of the microlithons was generally minor compared to the septa during cleavage formation and differentiation. Development of mica-rich septa and quartz-rich microlithons during the formation of a differentiated layering seems to be related to open-system mass transfer, at least in part, rather than just closed-system reorganization of elements between these two domains. Preservation locally of primary volcanic features in the microlithons and their homogeneous texture is consistent with this conclusion, although the evidence is equivocal.

On the basis of mass-balance calculations using Al as the immobile-element monitor, open-system solution-transfer development of fabric involved considerable leaching of silica (> 40 wt.%) with volume loss ($> 40\%$), assuming that the microlithons remained unchanged. The calculated degree of volume loss appears directly related to the original amount of quartz present in the rock, as was originally suspected. On the basis of simple calculations of solubility and assuming an open-system end-member scenario, the minimum metamorphic fluid:fabric ratio is on the order of 200. This

estimate of course becomes lower if the microlithons did not remain unchanged, *i.e.*, they may have been cryptically altered during deformation. The high fluid:rock values are reasonable, considering the high proportions of hydrated volcanic rocks and shales in the section. Furthermore, low-temperature metamorphic fluids evolved, at least in part, from sedimentary and volcanic rocks that were underplated and incorporated into a subduction complex at depths corresponding to the blueschist or high-pressure greenschist facies, over a considerably long period (van Staal 1994). This may be why differentiated layering and domainal cleavages are generally well developed in these settings (Bebout & Barton 1989, Williams 1990). Furthermore, the low-temperature metamorphic fluids that evolved from underplated sedimentary rocks in the accretionary wedge complex should be silica-unsaturated during buoyant migration and resultant heating through this part of the sequence, *i.e.*, the geothermal gradient was reversed. This could explain the high degree of silica mass-transfer from this part of the system, as well as the slightly lower $\delta^{18}\text{O}$ of the metamorphic fluids that resulted in isotopic depletion of ^{18}O within the fabrics.

Assuming that the microlithons were unchanged and open-system conditions prevailed, the major- and trace-element mobility was facilitated by hydrolysis and exchange reactions resulting from fluid advection and partial to complete reaction with the phyllosilicates. The stability of muscovite is enhanced within the foliation relative to feldspar at silica-unsaturated conditions, although slightly higher activities of Fe and Mg are required to stabilize chlorite through protolysis reactions. Overall, the changes in mass are minor, except for Fe and Zn, indicative of dissolution of disseminated sulfides from the fabrics and exchange with chlorite.

On average, residual enrichment of most high-ionic-potential elements (Ti, P, Ga, Y, and Nb), selected transition elements (Cr, V), and light rare-earth elements (*LREE*, La, Ce, Nd) within the septa are *nearly* directly proportional to Al abundance, attesting to their relative immobility during cleavage development. The relatively high proportion of accessory phases within the septa and overall coarser grain-size reflect fluid-enhanced growth.

ACKNOWLEDGEMENTS

I thank Ralph Kretz for his insight and guidance during my Ph.D. studies at the University of Ottawa (1987–1992). Bill Luff and the geological staff of Brunswick Mining and Smelting Limited are appreciated for their cooperation and encouragement with this study and continuing studies in the area. Discussions with Drs. Cees van Staal, Paul F. Williams, and Joseph C. White about fabric development were very helpful. This manuscript benefitted from comments by Drs. Cees van Staal, Paul Williams, Steve McCutcheon, Les Fyffe, and Neil Rogers and journal reviews by Eric Erslev and

Dan Kontak. This project is part of the five-year EXploration TECHnology (EXTECH II) federal-provincial Agreement.

REFERENCES

- AGUE, J.J. (1991): Evidence for major mass transfer and volume strain during regional metamorphism of pelites. *Geology* **19**, 855-858.
- ANDERSON, G.M. & BURNHAM, C.W. (1983): Feldspar solubility and the transport of aluminum under metamorphic conditions. *Am. J. Sci.* **283A**, 283-297.
- AYERS, J.C. & WATSON, E.B. (1991): Solubility of apatite, monazite, zircon, and rutile in supercritical aqueous fluids with implications for subduction zone geochemistry. *Philos. Trans. R. Soc. London A* **335**, 365-375.
- _____ & _____ (1993): Rutile solubility and mobility in supercritical fluids. *Contrib. Mineral. Petrol.* **114**, 321-330.
- BARNES, H.L. (1979): Solubilities of ore minerals. In *Geochemistry of Hydrothermal Ore Deposits* (second edition, H.L. Barnes, ed.). John Wiley & Sons Ltd., New York, N.Y. (404-460).
- BARRETT, T.J. & MACLEAN, W.H. (1994): Chemostratigraphy and hydrothermal alteration in exploration for VHMS deposits in greenstones and younger volcanic rocks. In *Alteration and Alteration Processes Associated with Ore-Forming Systems* (D.R. Lentz, ed.). *Geol. Assoc. Can., Short Course Notes* **11**, 433-467.
- BEACH, A. (1974): A geochemical investigation of pressure solution and the formation of veins in a deformed greywacke. *Contrib. Mineral. Petrol.* **46**, 61-68.
- _____ (1977): Vein arrays, hydraulic fractures and pressure solution structures in a deformed flysch sequence, S.W. England. *Tectonophysics* **40**, 201-225.
- _____ (1979): Pressure solution as a metamorphic process in deformed terrigenous sedimentary rocks. *Lithos* **12**, 51-58.
- BEBOUT, G.E. & BARTON, M.D. (1989): Fluid flow and metasomatism in a subduction zone hydrothermal system: Catalina Schist terrane, California. *Geology* **17**, 976-980.
- BELL, T.H. & CUFF, C. (1989): Dissolution, solution transfer, diffusion versus fluid flow and volume loss during deformation/metamorphism. *J. Metamorphic Geol.* **7**, 425-447.
- BHAGAT, S.S. & MARSHAK, S. (1990): Microlithon alteration associated with development of solution cleavage in argillaceous limestone: textural, trace-elemental and stable-isotopic observations. *J. Struct. Geol.* **12**, 165-175.
- BOWERS, T.S., JACKSON, K.J. & HELGESON, H.C. (1984): *Equilibrium Activity Diagrams for Coexisting Minerals and Aqueous Species at Pressures and Temperatures to 5 kb and 600°C*. Springer-Verlag, Berlin, Germany.
- BOYLE, R.W. & DAVIES, J.L. (1964): Geology of the Austin Brook and Brunswick No. 6 sulphide deposits, Gloucester County, New Brunswick. *Geol. Surv. Can., Pap.* **63-24**.
- BUCHER, K. & FREY, M. (1994): *Petrogenesis of Metamorphic Rocks*. Springer-Verlag, New York, N.Y.
- CLAYTON, R.N. & MAYEDA, T.K. (1963): The use of bromine pentafluoride in the extraction of oxygen from oxides and silicates for isotopic analysis. *Geochim. Cosmochim. Acta* **27**, 43-52.
- CONDIE, K.C. & SINHA, A.K. (1996): Rare earth and other trace element mobility during mylonitization: a comparison of the Brevard and Hope Valley shear zones in the Appalachian Mountains, USA. *J. Metamorphic Geol.* **14**, 213-226.
- COX, S.F. & ETHERIDGE, M.A. (1989): Coupled grain-scale dilatancy and mass transfer during deformation at high fluid pressures: examples from Mount Lyell, Tasmania. *J. Struct. Geol.* **11**, 147-162.
- CRERAR, D.A., SUSAK, N., BORCSIK, M. & SCHWARTZ, S. (1978): Solubility of the buffer assemblage pyrite + pyrrothite + magnetite in NaCl solutions from 200 to 350°C. *Geochim. Cosmochim. Acta* **42**, 1427-1437.
- DIPPLE, G.M. & FERRY, J.M. (1992a): Metasomatism and fluid flow in ductile fault zones. *Contrib. Mineral. Petrol.* **112**, 149-164.
- _____ & _____ (1992b): Fluid flow and stable isotopic alteration in rocks at elevated temperatures with applications to metamorphism. *Geochim. Cosmochim. Acta* **56**, 3539-3550.
- ERSLEV, E.A. (1998): Limited, localized nonvolatile element flux and volume change in Appalachian slates. *Geol. Soc. Am., Bull.* **110**, 900-915.
- _____ & WARD, D.J. (1994): Non-volatile element and volume flux in coalesced slaty cleavage. *J. Struct. Geol.* **16**, 531-553.
- ETHERIDGE, M.A., WALL, V.F., COX, S.F. & VERNON, R.H. (1984): High fluid pressures during regional metamorphism and deformation - implications for mass transport and deformation mechanisms. *J. Geophys. Res.* **89**, 4344-4358.
- _____ & VERNON, R.H. (1983): The role of the fluid phase during regional metamorphism and deformation. *J. Metamorphic Geol.* **1**, 205-226.
- EUGSTER, H.P. & ILTON, E.S. (1983): Mg-Fe fractionation in metamorphic environments. In *Kinetics and Equilibrium in Mineral Reactions* (S.K. Saxena, ed.). Springer-Verlag, New York, N.Y. (115-140).
- FERRY, J.M. (1981): Petrology of graphitic sulfide-rich schists from south-central Maine: an example of desulfidation during prograde regional metamorphism. *Am. Mineral.* **66**, 908-930.
- _____ (1994): A historical review of metamorphic fluid flow. *J. Geophys. Res.* **99**, 15487-15498.

- FOURNIER, R.O. (1985): The behavior of silica in hydrothermal solutions. In *Geology and Geochemistry of Epithermal Systems* (B.R. Berger & P.M. Bethke, eds.), *Rev. Econ. Geol.* **2**, 45-61.
- FUETEN, F., CLIFFORD, P.M., PRYER, L.L., THOMPSON, M.J., & CROCKET, J.H. (1986): Formation of spaced cleavage and concurrent mass removal of SiO₂. Meguma Group metagreywackes, Goldenville, Nova Scotia. *Maritime Sed. Atl. Geol.* **22**, 35-50.
- FYFE, W.S., PRICE, N.J. & THOMPSON, A.B. (1978): *Fluids in the Earth's Crust*. Elsevier, Amsterdam, The Netherlands.
- GLASSON, M.J. & KEAYS, R.R. (1978): Gold mobilization during cleavage development in sedimentary rocks from the auriferous Slate Belt of Central Victoria, Australia: some important boundary conditions. *Econ. Geol.* **73**, 496-511.
- GRANT, J.A. (1986): The isocon diagram – a simple solution to Gresens' equation for metasomatic alteration. *Econ. Geol.* **81**, 1976-1982.
- GRESENS, R.L. (1966): The effect of structurally produced pressure gradients on diffusion in rocks. *J. Geol.* **74**, 307-321.
- GUNTER, W.D. & EUGSTER, H.P. (1980): Mica-feldspar equilibria in supercritical alkali chloride solutions. *Contrib. Mineral. Petrol.* **75**, 235-250.
- HAACK, U., HEINRICHS, H., BONESS, M. & SCHNEIDER, A. (1984): Loss of metals from pelites during regional metamorphism. *Contrib. Mineral. Petrol.* **85**, 116-132.
- HEMLEY, J.J., CYGAN, G.L., FEIN, J.B., ROBINSON, G.R. & D'ANGELO, W.M. (1992): Hydrothermal ore-forming processes in the light of studies in rock-buffered systems. I. Iron – copper – zinc – lead sulfide solubility relations. *Econ. Geol.* **87**, 1-22.
- _____, MEYER, C., HODGSON, C.J. & THATCHER, A.B. (1967): Sulfide solubilities in alteration-controlled systems. *Science* **158**, 1580-1582.
- ILDEFONSE, J.-P. & GABIS, V. (1976): Experimental study of silica diffusion during metasomatic reactions in the presence of water at 550°C and 1000 bars. *Geochim. Cosmochim. Acta* **40**, 297-303.
- ILTON, E.S. & EUGSTER, H.P. (1990): Partitioning of base metals between silicates, oxides, and a chloride-rich hydrothermal fluid. I. Evaluation of data derived from experimental and natural assemblages. In *Fluid-Mineral Interactions: a Tribute to H.P. Eugster* (R.J. Spencer & I-Ming Chou, eds.), *The Geochemical Society, Spec. Publ.* **2**, 157-169.
- JENNER, G.A. (1996): Trace element geochemistry of igneous rocks: geochemical nomenclature and analytical geochemistry. In *Trace Element Geochemistry of Volcanic Rocks: Applications for Massive Sulphide Exploration* (D.A. Wyman, ed.), *Geol. Assoc. Can., Short Course Notes* **12**, 51-77.
- KERRICH, R. (1977): An historical review and synthesis of research on pressure solution. *Zentralbl. Palaont., Teil I*, 512-550.
- _____, FYFE, W.S., GORMAN, B.E. & ALLISON, I. (1977): Local modification of rock chemistry by deformation. *Contrib. Mineral. Petrol.* **65**, 183-190.
- KRETZ, R. (1983): Symbols for rock-forming minerals. *Am. Mineral.* **68**, 277-279.
- _____ (1994): *Metamorphic Crystallization*. John Wiley & Sons, New York, N.Y.
- LEITCH, C.H.B. & LENTZ, D.R. (1994): The Gresens' approach to mass balance constraints of alteration systems: methods, pitfalls, examples. In *Alteration and Alteration Processes Associated with Ore-forming Systems* (D.R. Lentz, ed.), *Geol. Assoc. Can., Short Course Notes* **11**, 161-192.
- LENTZ, D.R. (1995): Preliminary evaluation of six in-house rock geochemical standards from the Bathurst Camp, New Brunswick. In *Current Research 1994* (S.A. Merlini, ed.), *New Brunswick Department of Natural Resources and Energy, Minerals and Energy Division, Misc. Rep.* **18**, 81-89.
- _____ (1996): Trace-element systematics of felsic volcanic rocks associated with massive-sulphide deposits in the Bathurst Mining Camp: petrogenetic, tectonic and chemostratigraphic implications for VMS deposits. In *Trace Element Geochemistry of Volcanic Rocks: Applications for Massive Sulphide Exploration* (D.A. Wyman, ed.), *Geol. Assoc. Can., Short Course Notes* **12**, 359-402.
- _____ (1998): Petrogenetic evolution of felsic volcanic sequences associated with Phanerozoic volcanic-hosted massive sulphide systems: the role of extensional geodynamics. *Ore Geol. Rev.* **12**, 289-327.
- _____ (1999): Petrology, geochemistry, and oxygen isotope interpretation of felsic volcanic and related rocks hosting the Brunswick No. 6 and No. 12 massive sulfide deposits (Brunswick Belt) Bathurst Mining Camp, Canada. *Econ. Geol.* **94**, 57-86.
- _____ & GOODFELLOW, W.D. (1993): Petrology and mass-balance constraints on the origin of quartz-augen schist associated with the Brunswick massive sulfide deposits, Bathurst, New Brunswick. *Can. Mineral.* **31**, 877-903.
- _____ & _____ (1996): Intense silicification of footwall sedimentary rocks in the stockwork alteration zone beneath the Brunswick No. 12 massive sulphide deposit, Bathurst, New Brunswick. *Can. J. Earth Sci.* **33**, 284-302.
- _____, HALL, D.C. & HOY, L.D. (1997): Chemostratigraphic, alteration, and oxygen isotopic trends in a profile through the stratigraphic sequence hosting the Heath Steele B Zone massive sulfide deposit, New Brunswick. *Can. Mineral.* **35**, 841-874.
- LUFF, W.M., LENTZ, D.R. & VAN STAAL, C.R. (1993): The Brunswick No. 12 and No. 6 Mines, Bathurst Camp, north-

- ern New Brunswick. In *Guidebook to the Metallogeny of the Bathurst Camp* (S.R. McCutcheon & D.R. Lentz, eds.). Bathurst '93, Third Annual CIM Geological Field Conference, 75-105.
- LUSK, J. & KROUSE, H.R. (1997): Comparative stable isotope and temperature investigation of minerals and associated fluids in two regionally metamorphosed (Kuroko-type) volcanogenic massive sulfide deposits. *Chem. Geol.* **143**, 231-253.
- MANCKTELOW, N.S. (1994): On volume change and mass transport during the development of crenulation cleavage. *J. Struct. Geol.* **16**, 1217-1231.
- MASSONNE, H.-J. & SCHREYER, W. (1987): Phengite geobarometry based on the limiting assemblage with K-feldspar, phlogopite, and quartz. *Contrib. Mineral. Petrol.* **96**, 212-224.
- MCCLAY, K.R. (1977): Pressure solution and cobble creep in rocks and minerals: a review. *J. Geol. Soc. London* **134**, 57-70.
- MUELLER, R.F. (1967): Mobility of elements in metamorphism. *J. Geol.* **75**, 565-582.
- O'HARA, K. & BLACKBURN, W.H. (1989): Volume-loss model for trace-element enrichments in mylonites. *Geology* **17**, 524-527.
- O'NEIL, J.R. & TAYLOR, H.P., JR. (1969): Oxygen isotope fractionation between muscovite and water. *J. Geophys. Res.* **74**, 6012-6022.
- PARK, A.F. (1996): Structural evolution of sulphide tectonites and their host rocks, Stratmat mine, New Brunswick. *Can. J. Earth Sci.* **33**, 472-492.
- PEARCE, J.A., HARRIS, N.B.W. & TINDLE, A.G. (1984): Trace element discrimination diagrams for the tectonic interpretation of granitic rocks. *J. Petrol.* **25**, 956-983.
- DE ROO, J.A. & WILLIAMS, P.F. (1990): Dynamic recrystallization and solution transfer in mylonitic rocks of the Tetagouche Group, northern New Brunswick, Canada. *Geol. Soc. Am., Bull.* **102**, 1544-1554.
- ROYDEN, L.H. (1993): The steady state thermal structure of eroding orogenic belts and accretionary prisms. *J. Geophys. Res.* **98**, 4487-4507.
- RUTTER, E.H. (1983): Pressure solution in nature, theory and experiment. *J. Geol. Soc. London* **140**, 725-740.
- SACCOCIA, P.J., DING, K., BERNDT, M.E., SEEWALD, J.S. & SEYFRIED, W.E., JR. (1994): Experimental and theoretical perspectives on crustal alteration at mid-ocean ridges. In *Alteration and Alteration Processes Associated with Ore-forming Systems* (D.R. Lentz, ed.). *Geol. Assoc. Can., Short Course Notes* **11**, 403-431.
- SHAW, D.M. (1954): Trace elements in pelitic rocks. I. Variations during metamorphism. *Geol. Soc. Am., Bull.* **65**, 1151-1166.
- _____ (1956): Geochemistry of pelitic rocks. III. Major elements and general geochemistry. *Geol. Soc. Am., Bull.* **67**, 919-934.
- SPEAR, F.S. (1995): *Metamorphic Phase Equilibria and Pressure - Temperature - Time Paths*. Mineralogical Society of America, Washington, D.C., Monograph **1**.
- STEPHENS, M.B., GLASSON, M.J. & KEAYS, R.R. (1979): Structural and chemical aspects of metamorphic layering development in metasediments from Clunes, Australia. *Am. J. Sci.* **279**, 129-160.
- SVERJENSKY, D.A. (1985): The distribution of divalent trace elements between sulfides, oxides, silicates and hydrothermal solutions. I. Thermodynamic basis. *Geochim. Cosmochim. Acta* **49**, 853-864.
- VAN BAALEN, M.R. (1993): Titanium mobility in metamorphic systems: a review. *Chem. Geol.* **110**, 233-249.
- VAN STAAL, C.R. (1985): *The Structure and Metamorphism of the Brunswick Mines Area, Bathurst, New Brunswick, Canada*. Ph.D. thesis, Univ. of New Brunswick, Fredericton, New Brunswick.
- _____ (1987): Tectonic setting of the Tetagouche Group in northern New Brunswick: implications for plate tectonic models in the northern Appalachians. *Can. J. Earth Sci.* **24**, 1329-1351.
- _____ (1994): The Brunswick subduction complex in the Canadian Appalachians: record of the Late Ordovician to Late Silurian collision between Laurentia and the Gander margin of Avalon. *Tectonics* **13**, 946-962.
- _____ & FYFFE, L.R. (1995): Dunnage Zone - New Brunswick. In *Geology of the Appalachian-Caledonian Orogen in Canada and Greenland* (H. Williams, ed.). *Geol. Surv. Can., Geology of Canada* **6**, 166-178.
- _____, RAVENHURST, C.E., WINCHESTER, J.A., RODDICK, J.C., & LANGTON, J.P. (1990): Post-Taconic blueschist suture in the northern Appalachians of New Brunswick, Canada. *Geology* **18**, 1073-1077.
- _____ & WILLIAMS, P.F. (1984): Structure, origin and concentration of the Brunswick No. 12 and 6 orebodies. *Econ. Geol.* **79**, 1669-1692.
- WALTHER, J.V. & HELGESON, H.C. (1977): Calculation of the thermodynamic properties of aqueous silica and the solubility of quartz and its polymorphs at high pressures and temperatures. *Am. J. Sci.* **277**, 1315-1351.
- _____ & WOODLAND, A.B. (1993): Experimental determination and interpretation of the solubility of the assemblage microcline, muscovite, and quartz in supercritical H₂O. *Geochim. Cosmochim. Acta* **57**, 2431-2437.
- WENNER, D.B. & TAYLOR, H.P., JR. (1971): Temperatures of serpentinization of ultramafic rocks based on O¹⁸/O¹⁶ fractionation between coexisting serpentine and magnetite. *Contrib. Mineral. Petrol.* **32**, 165-185.

- WILLIAMS, P.F. (1972): Development of metamorphic layering and cleavage in low grade metamorphic rocks at Bermagui, Australia. *Am. J. Sci.* **272**, 1-47.
- _____ (1977): Foliation: a review and discussion. *Tectonophysics*. **39**, 305-328.
- _____ (1990): Differentiated layering in metamorphic rocks. *Earth-Sci. Rev.* **29**, 267-281.
- WINCHESTER, J.A. & FLOYD, P.A. (1977): Geochemical discrimination of different magma series and their differentiation products using immobile elements. *Chem. Geol.* **20**, 325-343.
- WINTSCH, R.P. (1985): The possible effects of deformation on chemical processes in metamorphic fault zones. In *Metamorphic Reactions, Kinetics, Textures, and Deformation* (A.B. Thompson & D.C. Rubie, eds.). Springer-Verlag, New York, N.Y. (251-268).
- _____ & DUNNING, J. (1985): The effect of dislocation density on the aqueous solubility of quartz and some geological implications: a theoretical approach. *J. Geophys. Res.* **90**, 3649-3657.
- _____, KVALE, C.M. & KISCH, H.J. (1991): Open-system, constant volume development of slaty cleavage, and strain-induced replacement reactions in the Martinsburg Formation, Lehigh Gap, Pennsylvania. *Geol. Soc. Am., Bull.* **103**, 916-927.
- WOOD, S.A. & WILLIAMS-JONES, A.E. (1994): The aqueous geochemistry of the rare-earth elements and yttrium. 4. Monazite solubility and REE mobility in exhalative massive-sulfide-depositing environments. *Chem. Geol.* **115**, 47-60.
- WRIGHT, T.O. & HENDERSON, J.R. (1992): Volume loss during cleavage formation in the Meguma Group, Nova Scotia, Canada. *J. Struct. Geol.* **14**, 281-290.

Received January 6, 1998, revised manuscript accepted March 15, 1999.